Journal of
Computational and Theoretical Nanoscience
Vol. 6, 1213–1235, 2009

Chemistry of Single-Walled Carbon Nanotubes

Charles See Yeung, Wei Quan Tian†, Lei Vincent Liu, and Yan Alexander Wang*

Department of Chemistry, University of British Columbia, Vancouver, BC V6T 1Z1, Canada

Single-walled carbon nanotubes (SWCNTs) have received significant attention from the scientific community over the past 15 years. Of particular interest is the potential of these macromolecules for use in molecular electronics, chemical sensory technology, nanobiology, and transition metal catalysis. For effective applications, the selective functionalization of the aforementioned all-carbon framework is necessary but has been met with considerable challenges. Herein, we review our approach to the exploration of structural and electronic properties of SWCNTs within density functional theory (DFT). Our investigations include mechanistic studies on chemical reactions of SWCNTs with defect and exploration of transition metal doped variants and their ability to adsorb small gas molecules.

Keywords: Single-Walled Carbon Nanotubes, Nanorods, Defect, Electronic Structure, Nitrogen Monoxide, Platinum, Gas Adsorption.

REVIEW

CONTENTS

1. Introduction 1213
2. SWCNTs 1217
2.1. Models and Computational Details 1217
2.2. Defected SWCNT Rods 1218
2.3. Pt-Doped SWCNT Rods with Fullerene Caps 1219
2.4. Pt-Doped SWCNT Rods with Hydrogen Caps 1222
3. Gas Adsorption onto Metal-Doped SWCNTs 1222
3.1. Adsorption of Carbon Monoxide 1222
3.2. Comparison with Alkylplatinum Complexes 1225
3.3. End-on Adsorption of Nitrogen-Based Gases: Nitrogen Monoxide, Ammonia, and Dinitrogen 1226
3.4. Adsorption of Hydrogen Gas 1227
3.5. Adsorption of Ethylene 1231
3.6. Adsorption of Acetylene 1232
3.7. Proposed Applications 1232
4. Concluding Remarks 1233
Acknowledgments 1233
References 1233

1. INTRODUCTION

The discovery of carbon nanotubes (CNTs) in 1991[1] and later, single-walled carbon nanotubes (SWCNTs),[2] can be considered two of the most significant contributions to the field of nanotechnology. Indeed, these unique allotropes of carbon have been the focus of significant attention in the scientific community in regards to their preparation, purification, and properties.[3,4] Both experimentalists and theorists alike have undertaken the challenge of investigating the utility of these macromolecules in applications including molecular electronics,[5–9] nanomechanics,[10,11] optics,[12,13] sensors,[5,14–18] and even catalysis.[19]

The molecular structure of SWCNTs can be thought of as an infinite graphene sheet rolled into a cylinder.[20,21] Figure 1 below illustrates the various means by which a graphite can be rolled into a nanotube.[22] SWCNTs are typically classified as metallic or semiconducting depending on the diameter and chirality of the tube.[22,23] Locally, each C atom residing in the cylinder exhibits partial sp^3 character[20] with slight misalignment of π-orbitals between adjacent atoms.[22]

One prominent use of CNTs is as the filler for polymer nanocomposites.[24–29] These multiphase materials contain a homogeneous dispersion of an ultrafine component[30] that can modify the mechanical, electronic, rheological and thermal properties of the unfilled polymer.[20] Much lower constituent loadings (*cf.* 0.1 wt% or less)[20] than traditional fillers (*cf.* 15–40 wt%) are required to achieve the same property enhancements.[30] Importantly, CNTs have been shown to impart enhanced rigidity, optical clarity, and electrical conductivity.[30] In fact, polymer matrices that are insulating but contain conductive nanoparticles can become conductive above a certain filler concentration known as the percolation threshold,[20] as low as 0.005 vol% in the case of a SWCNT/epoxy composite.[24] Percolation thresholds are strongly dependent on aspect ratio,[24] dispersion,[24,26,27,31] and alignment.[25,28,29]

*Author to whom correspondence should be addressed.
†Permanent address: State Key Laboratory of Theoretical and Computational Chemistry, Institute of Theoretical Chemistry, Jilin University, Jilin 130023, China.

Charles S. Yeung was born in Hong Kong in 1984 and immigrated to Canada when he was 5. In 2006, he received his B.Sc. degree in honours chemistry from the University of British Columbia under the supervision of Professor Laurel Schafer. The following summer, Charles began investigating single-walled carbon nanotubes in the laboratory of Professor Alex Wang. He is currently a Ph.D. candidate in the Dong Research Group at the University of Toronto. His research focuses on the development of new transition metal catalyzed strategies for the utilization of carbon dioxide as a renewable feedstock for organic synthesis. Charles is the recipient of an NSERC Julie Payette Research Scholarship and an NSERC Canada Graduate Scholarship (Ph.D.).

Wei Quan Tian was born in Chongqing, China, in 1971. He obtained his B.Sc. (1994) and M.Sc. (1997) degrees from Jilin University in China. In 2001, he received his Ph.D. degree in physical chemistry from the University of Guelph under the supervision of Professor John D. Goddard. In the next three years, he gained his postdoctoral research experience with Professor Alain St-Amant at the University of Ottawa and Professor Alex Wang at the University of British Columbia. In 2004, he took a Japan Society for the Promotion of Sciences fellowship working in the group of Professor Yuriko Aoki at Kyushu University. After the JSPS fellowship, he then joined the Institute of Theoretical Chemistry at Jilin University as a full professor. He was a visiting professor of physics at the University of Louisville working with Professor Shi-Yu Wu. His research interests range from chemical reaction mechanism, molecular dynamics, optoelectronics, non-linear optics, nano-materials, to simulation method development. He has co-authored around 70 publications including book chapters and review articles.

Lei Liu was born in Zigong, Sichuan Province, China, in 1980. He received a B.Sc. degree in Chemistry from Bejing Normal University in 2003 and a M.Sc. degree in Computational Chemistry from the University of British Columbia in 2006 under the supervision of Professor Alex Wang. He is a Ph.D. student at Stanford University and is using spectroscopic and theoretical methods to study mono-nuclear non-heme iron enzymes under the guidance of Professor Edward Solomon. He received the Gladys Estella Laird and Charles A. McDowell fellowships when he was at the University of British Columbia.

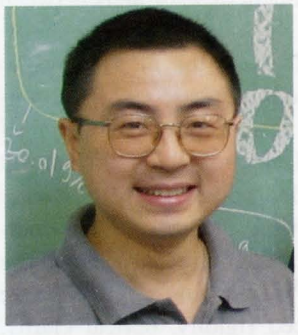

Alex Wang was born in Shashi, Hubei Province, China, in 1971. He is a tenured Associate Professor of Chemistry at the University of British Columbia. He obtained his B.Sc. degree in Organic Chemistry at Jilin University in 1991 and received his Ph.D. degree in Chemical Physics from Indiana University at Bloomington in 1995 under the supervision of Professor Ernest R. Davidson. He was a postdoctoral fellow at the University of North Carolina at Chapel Hill with Professor Robert G. Parr from 1995 to 1997 and UCLA with Professor Emily A. Carter from 1997 to 2001. Since joining UBC in 2001, he has been actively conducting his research in the three fronts of theoretical chemistry: fundamental theory, method development, and state-of-the-art applications, including deeper understanding of functional derivative and chemical potential, revitalizing orbital-free density functional theory, and unveiling mechanisms of important chemical reactions in nanomaterials and synthetic chemistry. He received the Wiley Young Investigator Award at the 47th Sanibel Symposium in 2007 and UCLA Chancellor's Postdoctoral Research Award in 2001. He is a member of Board of Advisors of the *International Association of Scientists in the Interdisciplinary Areas* and is a member of the Editorial Boards of *Interdisciplinary Sciences: Computational Life Sciences, Progress in Theoretical Chemistry and Physics*, and *The Journal of Computational and Theoretical Nanoscience*. He has published over 60 papers and has given 25 invited talks at international and national conferences.

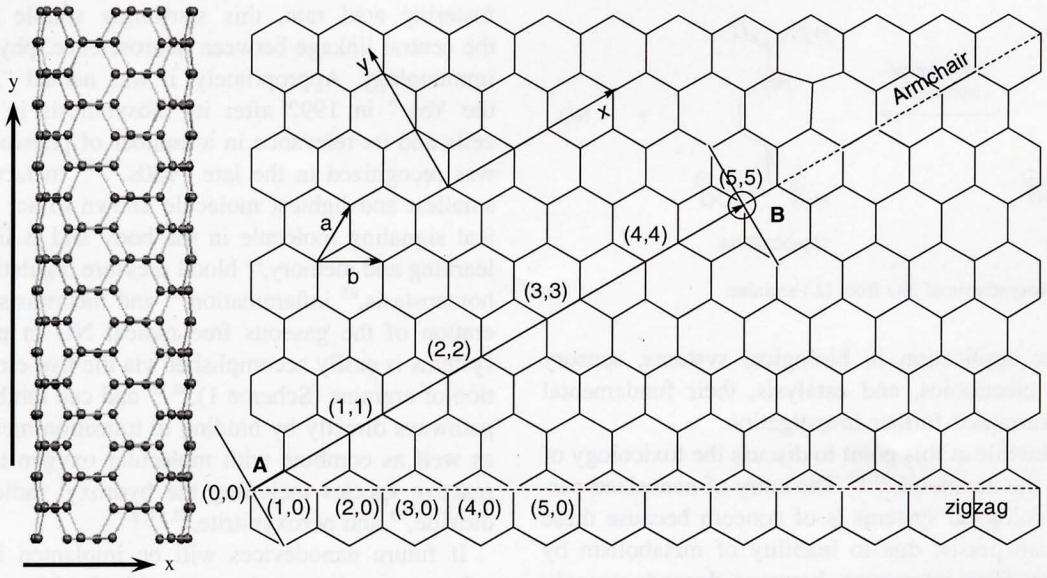

Fig. 1. A schematic illustrating the wrapping of a graphene sheet to form a SWCNT. A segment of the (5, 5) SWCNT is shown on the left.

Yodh and co-workers[24] recently studied the conductivity thresholds in an epoxy-based nanocomposite and found that SWCNTs with lower aspect ratios gave higher percolation thresholds.[20, 24] This group also showed that dispersion affected the observed values by examining the effect of sonication of the SWCNT/polymer composites prior to curing.[24] Since well-dispersed SWCNTs have a higher aspect ratio than aggregates, one might expect that this pretreatment should yield lower percolating thresholds,[20, 27] but it is also known that interaction between the filler particles themselves play a role in the formation of conductive networks,[24] specifically nanotube–nanotube contact resistance.[26, 32] The effect of alignment in the electrical conductivity of polymer nanocomposites has also been investigated, where it is believed that a more ordered arrangement of the ultrafine phase results in a reduction in the number of contacts between the nanotubes and hence an increased percolation threshold.[20] Indeed, Winey and co-workers have shown through both experiment and theory that SWCNT/poly(methyl methacrylate) composites support this hypothesis.[25, 28]

Because of the large level of delocalization of electrons in the extended π-system of SWCNTs,[20, 22, 23] mean free paths on the order of a micron have been suggested.[33] Chemical functionalization can easily disrupt the extended conjugation and reduce the electrical conductivity along the axis of the tube. Within a polymer matrix, however, the dependence of conductance on functionalization can be reversed, since the steric and electronic properties of the nanotubes affect aspect ratio, dispersion, and alignment of the filler (*vida supra*).[20] For instance, amine,[34] amide,[35] hydroxyl, and carboxyl groups[36] have each been successfully added to the sidewall of SWCNTs within a polymer matrix and imparted improved electrical properties in comparison to the isolated macromolecules.

Many groups have attempted to achieve selective functionalization of SWCNTs: tandem fluorination/nucleophilic substitution,[37, 38] carbene addition,[39] dipolar cycloaddition of azomethine ylides,[40] nitrene addition,[41] Lewis acid-catalyzed electrophilic addition,[42] dissolving metal reduction (Billups reaction),[43] and hydroboration.[44] Reactivity, though, is often difficult to control and characterization proves equally challenging. Doping is an alternative, yielding a hetero-SWCNT (HSWCNT). Both B- and N-doped SWCNTs have been synthesized by thermal treatment,[45] chemical vapor deposition,[46] laser ablation,[47] and the arc method,[48] but with poor control of doping position and concentration.[49–51] In 2004, Srivastava et al.[52] proposed that a free gas-phase neutral N atom, if brought into close vicinity with a vacancy in the C backbone, can induce a substitution process to occur. Later, our group proposed the use of NO as a nitrogen source.[50] The doping of the sidewall of SWCNTs with transition metals, however, remains to be achieved[22, 23, 49, 53–57] despite the fact that the closely-related transition metal-doped fullerenes have been prepared.[58–62] Cage substitution can take place by evaporation of pure metals followed by heating[58] or laser ablation.[59, 60] In all of these cases, the energy gap between the highest occupied molecular orbital (HOMO) and the lowest unoccupied molecular orbital (LUMO) decreases in comparison to C_{60} upon the introduction of a transition metal atom into the cage,[61] resulting in higher conductivity[61] and reactivity[62] and hence suggests similar effects for nanotubes.[23]

We became interested in SWCNTs and their interaction with small molecules because of the rich chemistry of these macromolecules. In particular, the unique reactivity made possible by imperfections in nanotube structure[49, 50] and doping with a non-carbon atom caught our attention.[22, 23, 49, 63, 64] Since nanomaterials have the

REVIEW

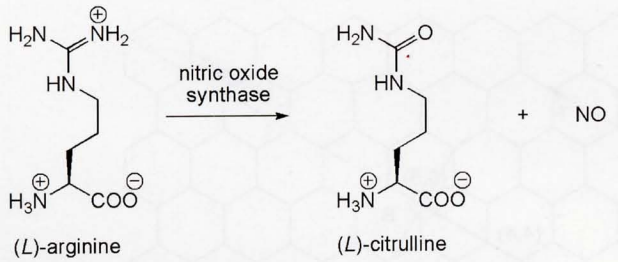

Scheme 1. Biosynthesis of NO from (*L*)-arginine.

potential for application in biological systems, sensory technology, electronics, and catalysis, their fundamental chemistry warranted further investigation.

It is worthwhile at this point to discuss the toxicology of materials at the nanolevel.[65–69] The entry of nanosized particles into biological systems is of concern because these molecules can persist due to inability of metabolism by macrophages. Their interaction, however, depends strongly on the particle size, surface charge, and surface area, each of which affects the agglomeration of particles and in turn the diffusion of these species through biological environments.[66] The main mode of toxicity is believed to be oxidative stress induced by the generation of reactive oxygen species (ROS).[65, 66, 70–72] Because of the often extended nature of nanomaterials, the presence of ultraviolet light may induce the formation of an electron–hole pair and the subsequent creation of a radical that can oxidize molecular oxygen to superoxide, for instance. These types of processes can also take place through electron-active groups either due to defects or surface coatings.[65, 66] Over time, the accumulation of ROS depletes the natural antioxidant defenses such as glutathione,[73] and force cells to respond by more drastic measures.[71–73] Cytotoxicity of carbon-based nanomaterials has been observed for human skin fibroblasts,[74] macrophages,[75, 76] and developing zebrafish embryos.[77] While no clinically relevant toxicity has been reported,[66] the concern among researchers is a real one.

Toxicology aside, nanomaterials truly have great potential benefits as well. Consider NO for a moment. Nitrogen is one of the most important elements in biological systems[78] and among its seven known oxides, nitric oxide deserves special attention. Despite its reputation as the toxic culprit for destroying ozone, causing cancer, and fostering acid rain, this startlingly simple molecule is the central linkage between neuroscience, physiology, and immunology. Appropriately, it was named "Molecule of the Year" in 1992 after its biosynthesis in mammalian cells and its relevance in a number of physiological roles was recognized in the late 1980s.[79, 80] In fact, NO is the smallest and lightest molecule known to act as a biological signaling molecule in the body and is important for learning and memory,[81] blood pressure regulation,[81, 82] skin homeostasis,[83] inflammation,[84] and metastasis.[85] The generation of the gaseous free radical NO in physiological systems is easily accomplished via the five-electron oxidation of arginine (Scheme 1),[80, 86] and can inhibit metabolic pathways directly by binding to transition metal centers,[87] as well as combine with molecular oxygen to give other reactive species including the hydroxyl radical, nitrogen dioxide,[79] and peroxynitrite.[80, 81, 87]

If future nanodevices will be implanted into biological systems, it may interact with the biocycles of NO. The ability to adsorb NO would be important because it would reduce the concentration near the proximity of the material and can be either beneficial or dangerous depending on the site of activity. The release of NO is also significant, illustrated through recent research aimed at chemically-designed drugs (Fig. 2),[80] zeolites,[88, 89] or even Pt nanoparticles;[90] CNTs would be an alternative.

The interaction with small molecules may further be enhanced in the case of transition metal-doped nanotubes since it is well known that metal surfaces and organometallic complexes alike can bind small molecules.[91–95] Apart from applications in biology, nanomaterials may also act as sensors. Namely, since the adsorption of gases onto the HSWCNT would result in a charge transfer[96, 97] and conductivity variation,[49] the observed conductance can be used as an analytical parameter. Although the idea of using nanotubes as sensors for gases is not new,[96–100] expansion of the scope to simple molecules such as CO, H_2O, and H_2 [97, 101] has attracted the attention of research groups around the world. In fact, while dispersion of Pd nanoparticles onto the surface of SWCNTs,[94] doping with B and N,[97] and physical deformation of the suprastructure[101] have all been considered, our hypothetical HSWCNTs could also work. Furthermore, since adsorption would represent a reversible electronic tuning of nanotubes, employment in nanoelectronics are possible as well.

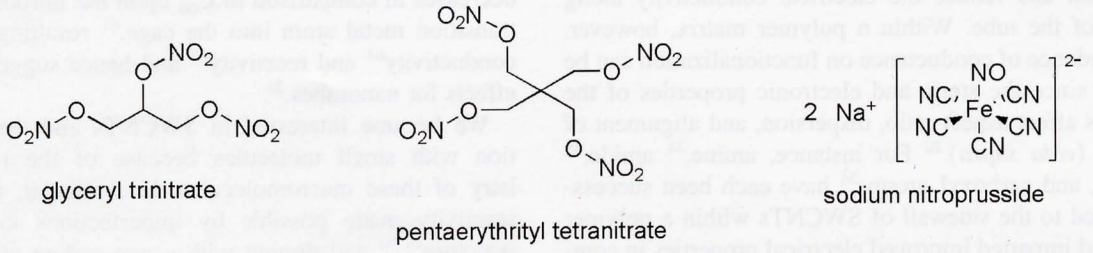

Fig. 2. Clinically used NO donor drugs.

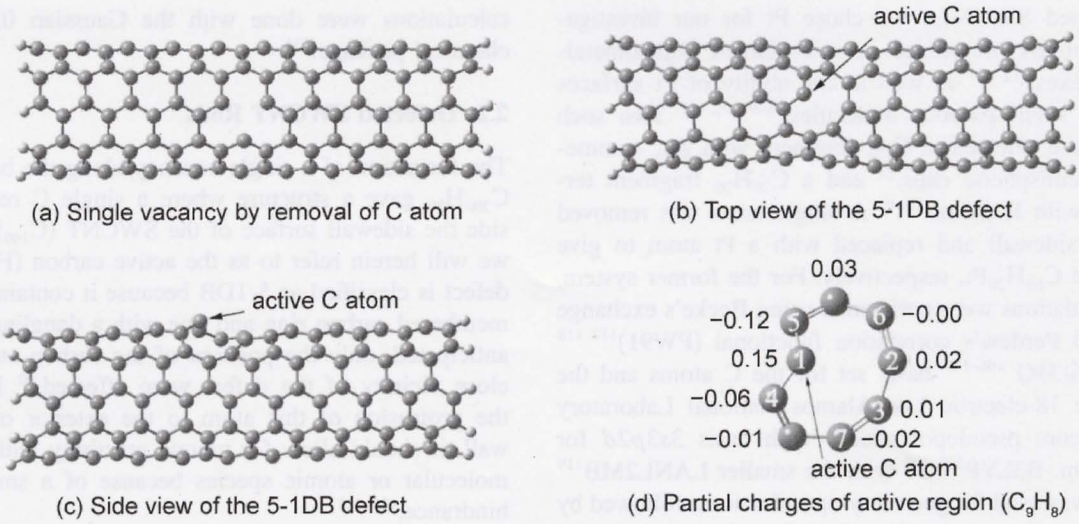

Fig. 3. 5-1DB defected SWCNT.

In this review, we will show some results from our studies of the structure and electronic properties of defected and doped SWCNTs and their chemical reactivity with small gas molecules. Such investigative efforts should constitute the first step towards a microscopic understanding of the toxicology of nanomaterials in the human body and the development and discovery of new materials with exciting applications in the real world.

2. SWCNTs

2.1. Models and Computational Details

The (5, 5) armchair metallic SWCNT was used as a model for all computations. For the investigation of the defected SWCNT, a segment containing 200 carbon atoms and 20 capping hydrogen atoms was chosen ($C_{200}H_{20}$). A single vacancy was then created by removal of a single carbon atom, yielding a metastable conformation with three dangling bonds (DBs).[50] Geometry optimization was achieved sequentially with the semiempirical MNDO-PM3 method,[102] followed by the hybrid Hartree-Fock/density functional theory (DFT) method B3LYP[103–105] with Pople's 6-31G basis set.[106–109] The nine-membered ring surrounding the defect was considered to be the chemically active region and modeled appropriately with a C_9H_8 fragment for the higher layer of a two-layered ONIOM model,[110] treated at the B3LYP/6-31G(d) level of theory. All other carbon atoms in the lower layer were treated by the universal force field (UFF).[111]

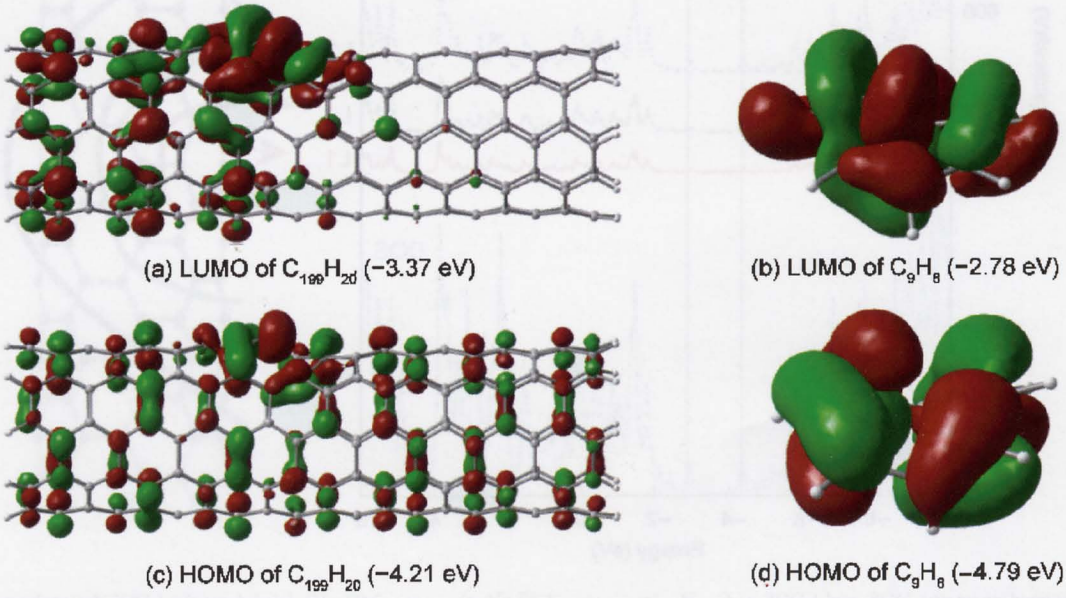

Fig. 4. FMOs of $C_{199}H_{20}$ and higher-layer model C_9H_8. Orbital energies are in parentheses.

For doped SWCNTs, we chose Pt for our investigation due to its prevalence in well-defined organometallic complexes,[112–114] as well as the ability of Pt surfaces to adsorb small gaseous molecules.[91–93, 95, 115] Two such models were selected: a C_{170} fragment with D_{5h} symmetry and hemispheric caps,[22] and a $C_{70}H_{20}$ fragment terminating with H atoms.[23, 49] A single atom was removed from the sidewall and replaced with a Pt atom to give $C_{169}Pt$ and $C_{69}H_{20}Pt$, respectively. For the former system, DFT calculations were performed using Becke's exchange (B)[116] and Perdew's correlation functional (PW91)[117, 118] with the 6-31G [106–109] basis set for the C atoms and the relativistic 18-electron Los Alamos National Laboratory effective core pseudopotential[119] with basis $3s3p2d$ for the Pt atom. B3LYP[103–105] with the smaller LANL2MB[119] basis set was used for geometry optimizations, followed by refinement with the larger LANL2DZ basis. For $C_{69}H_{20}Pt$, the exchange-correlation density functional of Perdew, Burke, and Ernzerhof (PBEPBE)[120] was employed using the same basis sets. Natural bond orbital (NBO) analyses were accomplished with Gaussian NBO Version 3.1,[121, 122] while density of states (DOS) and local DOS (LDOS) studies were performed using PyMOlyze.[123] All other calculations were done with the Gaussian 03 quantum chemical package.[124]

2.2. Defected SWCNT Rods

The formation of a single vacancy along the backbone of $C_{200}H_{20}$ gave a structure where a single C remains outside the sidewall surface of the SWCNT ($C_{199}H_{20}$) which we will herein refer to as the active carbon (Fig. 3). The defect is classified as 5-1DB because it contains one five-membered carbon ring and one with a dangling bond. As anticipated, only the position of the carbon atoms in the close vicinity of the defect were affected.[50] Because of the protrusion of this atom to the exterior of the sidewall, it should allow for unique reactivity with incoming molecular or atomic species because of a smaller steric hindrance.[125–127]

Single-point energy calculations revealed that the HOMO–LUMO gap decreased from 1.38 to 0.84 eV upon the introduction of the defect, suggesting a destabilization of the HOMO and stabilization of the LUMO. The HOMO contains a large contribution from the lone-pair of electrons on the active carbon atom and the π-bonds of the other atoms within the nine-membered ring highlighted

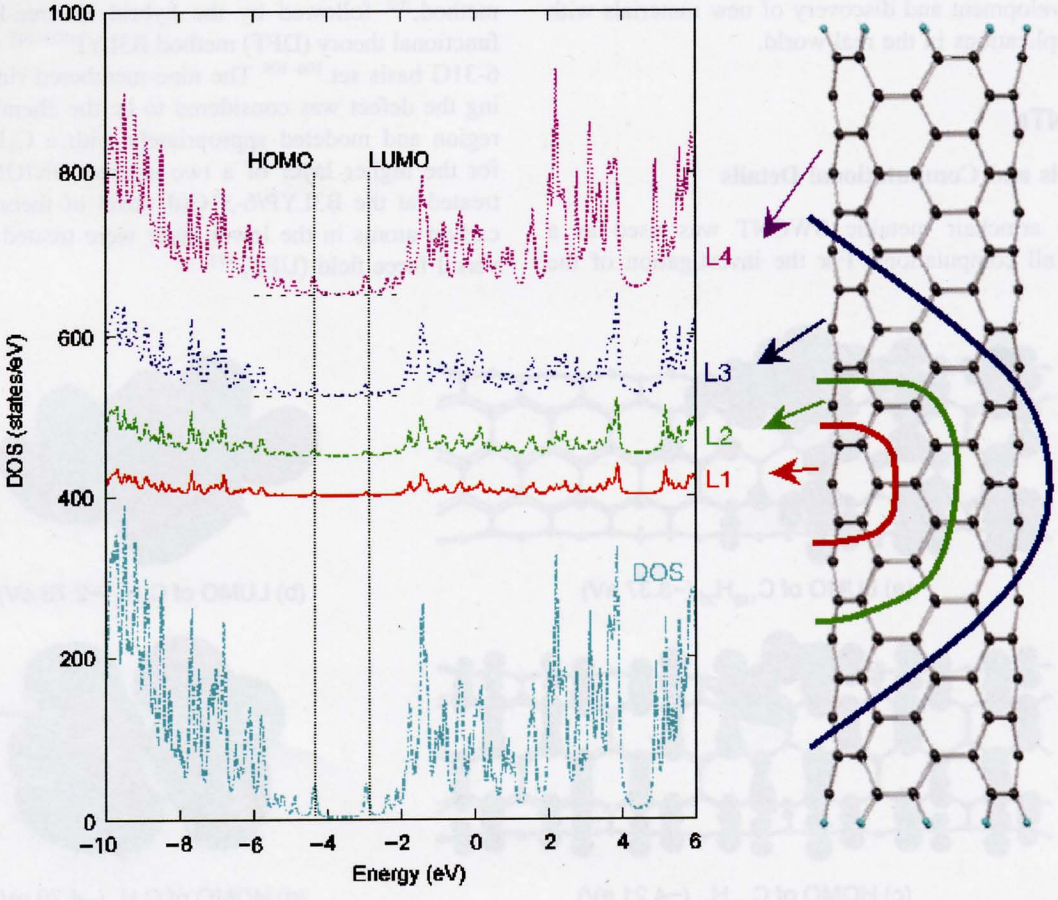

Fig. 5. Optimized geometry, DOS, and LDOS of $C_{200}H_{20}$ ($\varepsilon_{HOMO} = -4.35$ eV, $\varepsilon_{LUMO} = -2.97$ eV). L1–L4 are the LDOS for each specified layer of atoms as marked on the diagram.

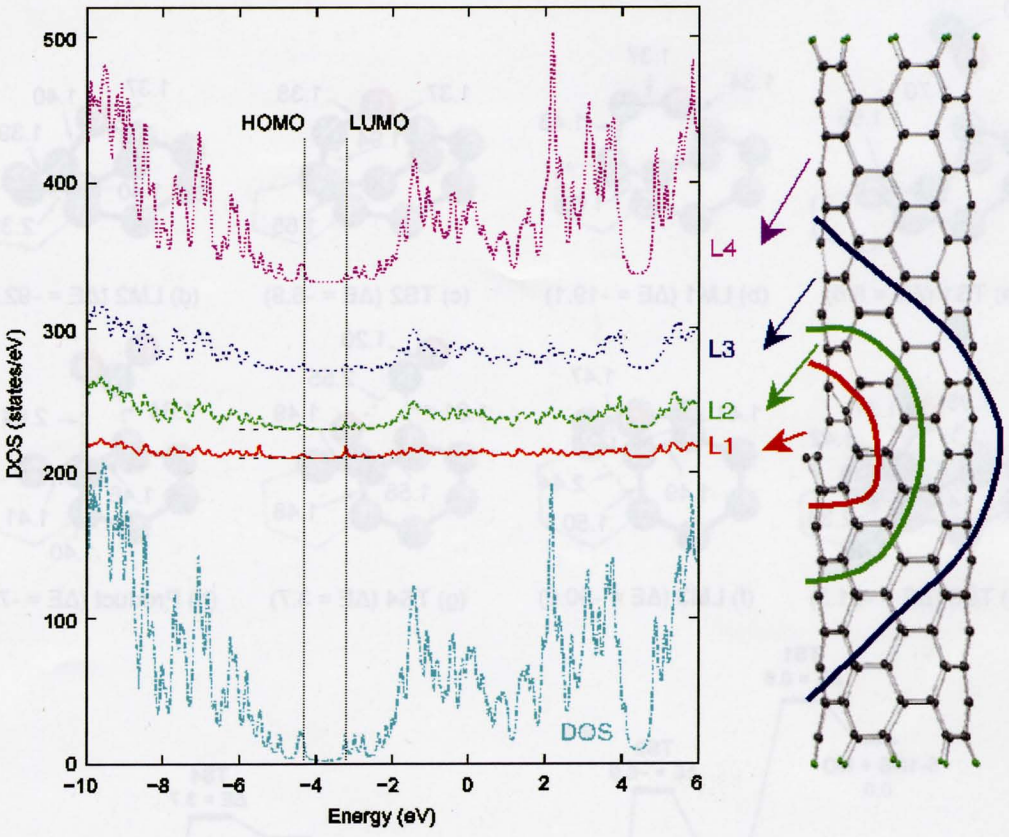

Fig. 6. Optimized geometry, DOS, and LDOS of $C_{199}H_{20}$ ($\varepsilon_{HOMO} = -4.21$ eV, $\varepsilon_{LUMO} = -3.37$ eV). L1–L4 are the LDOS for each specified layer of atoms as marked on the diagram.

in Figure 3(d), considered to be the active region in the macromolecule as validated by the frontier molecular orbitals (FMOs) and the LDOS (Figs. 4–6).[50]

Taking the nine-atom C_9H_8 as a model of the 5-1DB defect, our ONIOM model predicted interaction with the small molecule NO via the pathway shown in Figure 7.[50] A NBO analysis revealed occupation of an $sp^{2.01}$-orbital with 1.51 electrons and a p-orbital with 0.51 electrons on the active carbon and an overall charge of 0.149. Indeed, the O-end attack produced an appropriate transition state where it is the electrostatic effect that appears to be of the greatest importance, producing the first intermediate, **LM1**. The barrier to this process is merely 8.6 kcal mol^{-1}. In a classical sense, this type of reaction can be considered to be the result of interaction between the singly-occupied molecular orbital of NO with the HOMO of the defected SWCNT.[50]

With the formal adsorption of NO via bond formation between C1 and O and between C2 and N, an insertion then takes place on the pentagon, resulting in the elongation of the C2–C3 bond length and the release of a further 73.3 kcal mol^{-1}. Finally, the C1–O bond is cleaved in favor of the formation of a C1–N bond, yielding an N-oxide radical with the N filling the single vacancy that was removed. This product is 90.0 kcal mol^{-1} more stable than the reactants and suggests that the net reaction of NO with $C_{199}H_{20}$ is thermodynamically feasible.[50]

In the presence of excess NO, however, a further reaction may take place. The length of the N–O bond is 1.41 Å in **LM3**, with the unpaired electron localized mainly on the O atom, exhibiting a −0.574 partial charge. The electron density on the O atom appears to direct a second molecule of NO to interact with C1 via the N atom to ultimately give a molecule of NO_2 bound to C1 with a bond length of 1.64 Å between C1 and the adsorbate. The formation of the final product is exothermic from the NO–SWCNT complex (78.3 kcal mol^{-1}) through a very low barrier (3.7 kcal mol^{-1}). It is the case, therefore, that NO acts as a reducing agent to remove the O atom and yield NO_2 and a N-doped SWCNT through a one-step reaction. The HOMO–LUMO gap for this final product is only 0.74 eV, decreased from both the perfect and defected SWCNTs.[50]

2.3. Pt-Doped SWCNT Rods with Fullerene Caps

The substitution of a single C atom with Pt is possible in three distinct manners for the SWCNT segment with fullerene caps (Fig. 8): cap-end-doped $C_{169}Pt(ce)$, cap-doped $C_{169}Pt(c)$, and wall-doped $C_{169}Pt(w)$.[22] Geometry optimization reveals that the transition metal tends to protrude to the exterior of the sidewall of the nanotube, adopting a conformation where the three nearest

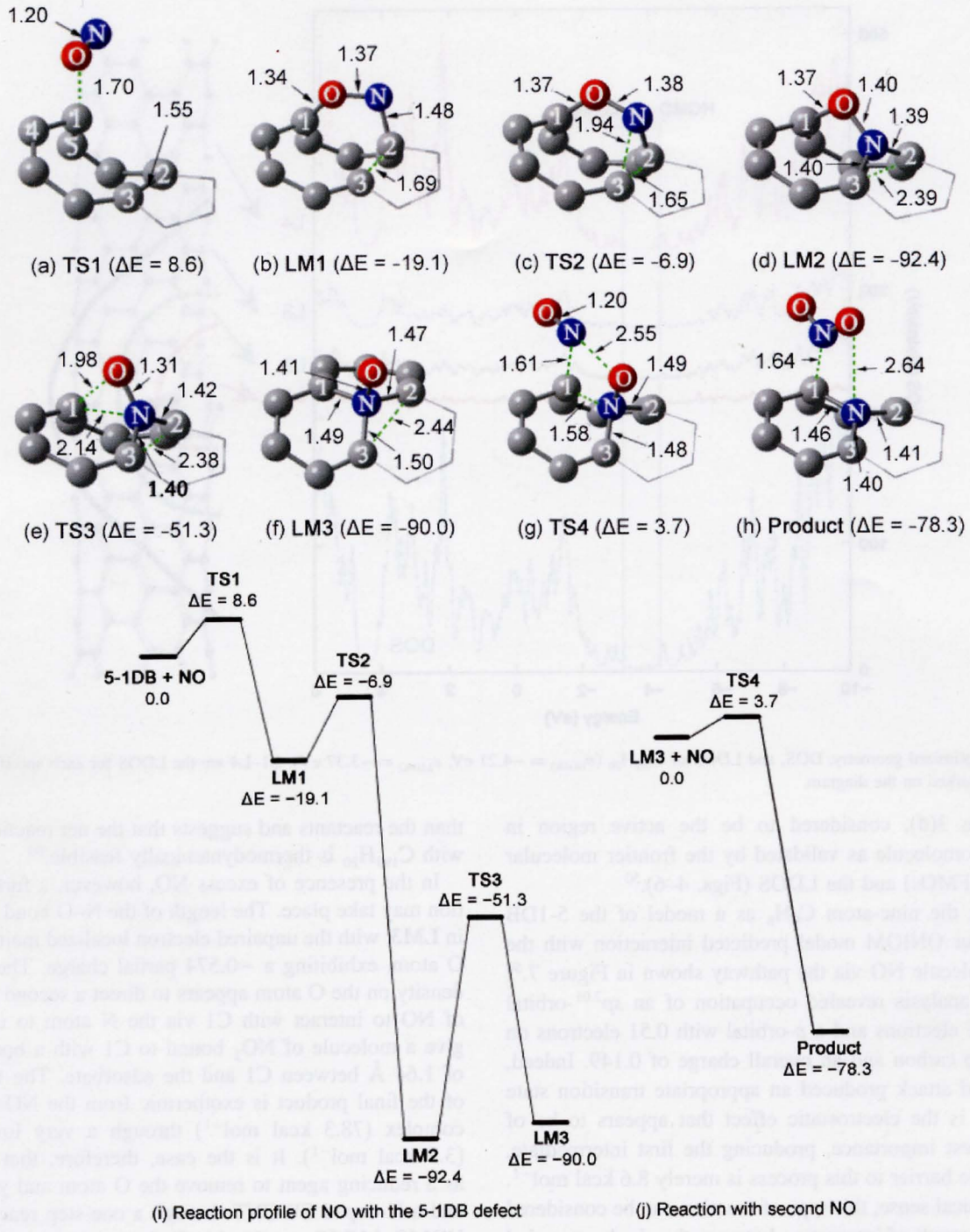

Fig. 7. Optimized geometries (with distances in Å) and energy profiles (with energies in kcal mol^{-1}) for the reaction of the defected SWCNT with NO.

neighbor C atoms are positioned in a tripod-like fashion. At the BPW91/6-31G level of theory, $C_{169}Pt(ce)$ is the most stable of the three, where the energies of $C_{169}Pt(c)$ and $C_{169}Pt(w)$ are 0.8 and 17.9 kcal mol^{-1}, respectively, above that of $C_{169}Pt(ce)$. In all scenarios, the singlet electronic state was found to be lower in energy than the triplet, suggesting that the ground state of the nanorod is singlet.[22]

The optimized geometry, DOS, LDOS, and relevant molecular orbitals (MOs) of $C_{169}Pt(ce)$ are shown in Figures 9 and 12. The Pt and C atoms at the cap end are separated by 2.01 Å (*cf.* 1.73 Å for the isolated PtC molecule[23]). We suspect that the reason for the low energy of $C_{169}Pt(ce)$ is the relaxation of the constraint on the cap through doping. However, significant distortion of the SWCNT can be clearly seen on the pentagons and

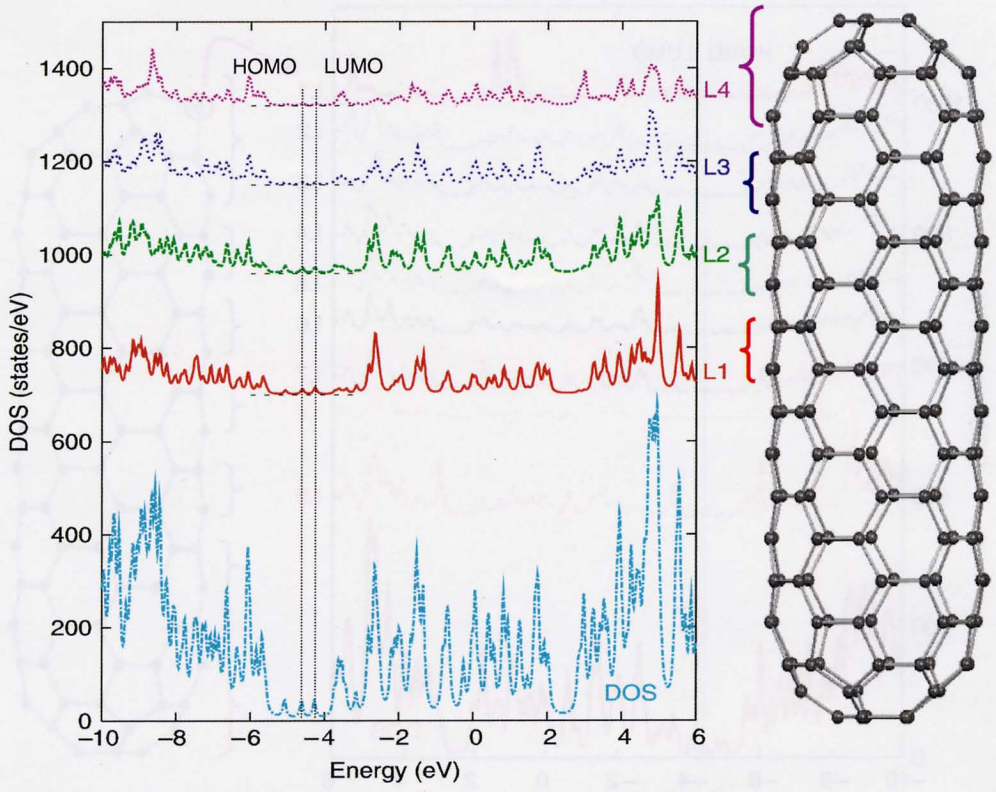

Fig. 8. Optimized geometry, DOS, and LDOS of C_{170} with D_{5h} symmetry ($\varepsilon_{HOMO} = -4.61$ eV, $\varepsilon_{LUMO} = -4.26$ eV). L1–L4 are the LDOS for each specified layer of atoms as marked on the diagram.

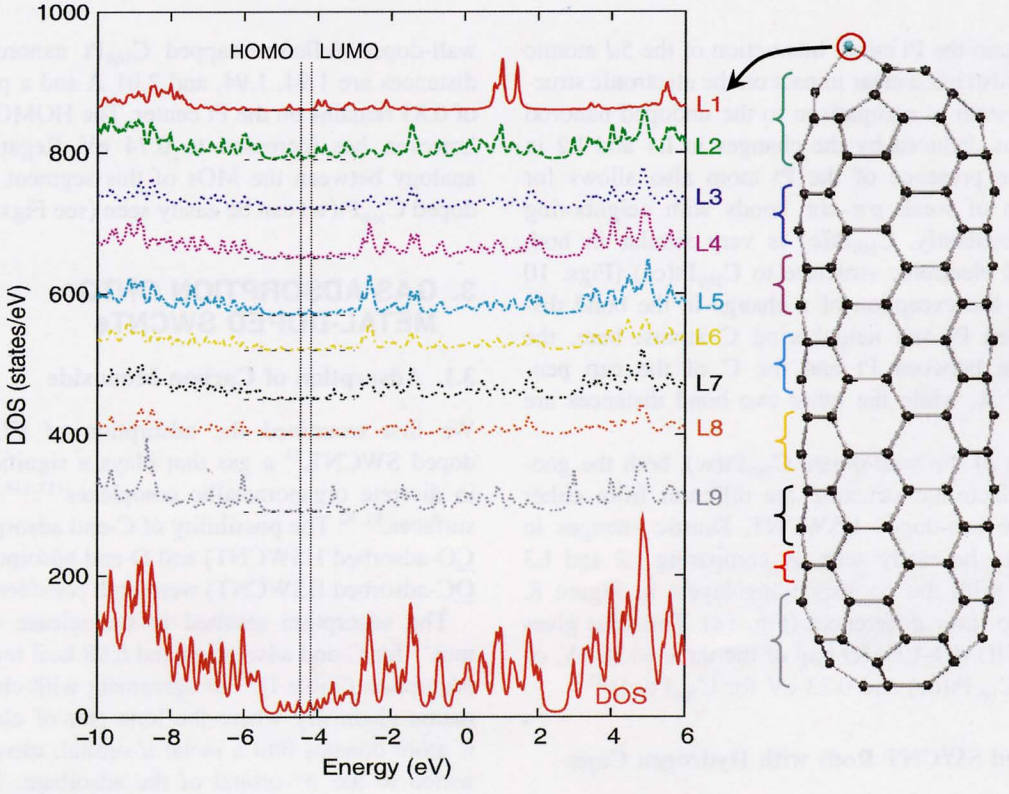

Fig. 9. Optimized geometry, DOS, and LDOS of $C_{169}Pt(ce)$ with C_s symmetry ($\varepsilon_{HOMO} = -4.51$ eV, $\varepsilon_{LUMO} = -4.21$ eV). L1-L9 are the LDOS for each specified layer of atoms as marked on the diagram.

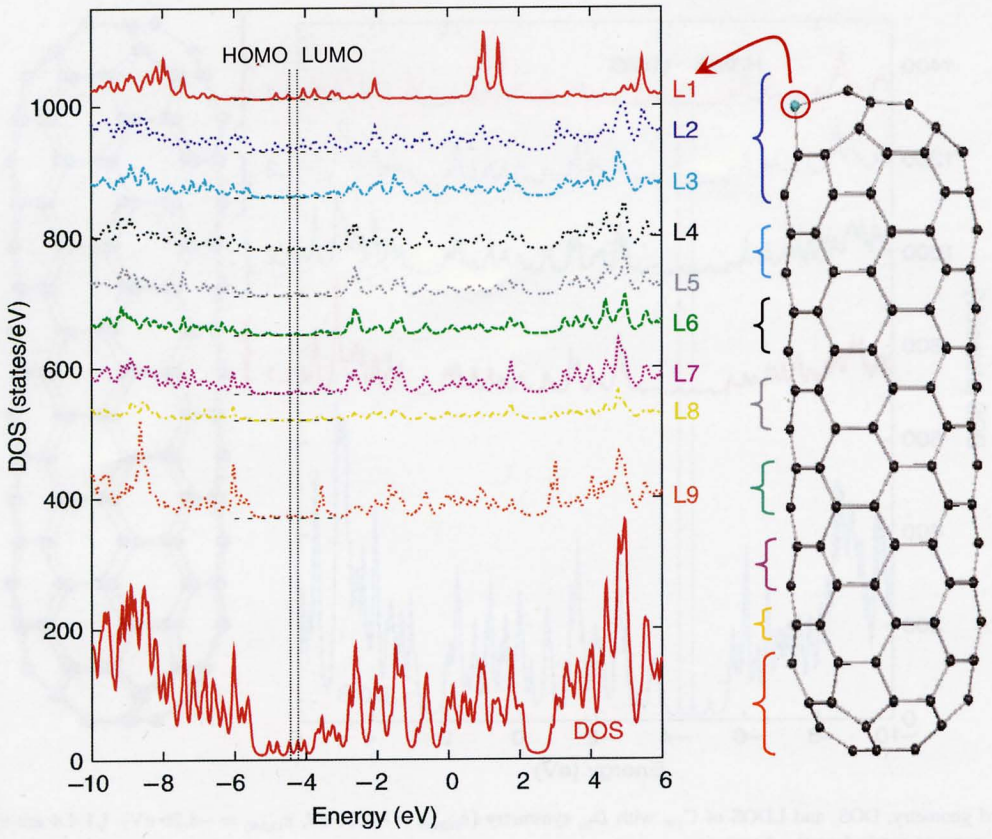

Fig. 10. Optimized geometry, DOS, and LDOS of $C_{169}Pt(c)$ with C_s symmetry ($\varepsilon_{HOMO} = -4.48$ eV, $\varepsilon_{LUMO} = -4.25$ eV). L1–L9 are the LDOS for each specified layer of atoms as marked on the diagram.

hexagons around the Pt atom. Interaction of the 5*d* atomic orbitals of Pt also has a clear impact on the electronic structure of the system in comparison to the undoped nanorod (see Fig. 8) as deduced by the changes in L1 and L2 in Figure 9. The presence of the Pt atom also allows for the formation of weak $p\pi$–$d\pi$ bonds with neighboring C atoms.[22] Evidently, $C_{169}Pt(c)$ is very similar in both geometry and electronic structure to $C_{169}Pt(ce)$ (Figs. 10 and 13) with the exception of a change in the bond distances between Pt and neighboring C atoms: here, the bond distance between Pt and the C of the cap pentagon is 1.97 Å, while the other two bond distances are 2.00 Å.[22]

In the case of the wall-doped $C_{169}Pt(w)$, both the geometric and electronic structure are different from either variant of the cap-doped HSWCNT. Drastic changes in the LDOS can be easily seen by comparing L2 and L3 in Figure 11 with the corresponding layers in Figure 8. The MOs also show differences (Fig. 14). This case gives the smallest HOMO–LUMO gap of the three (0.20 eV, *cf.* 0.30 eV for $C_{169}Pt(ce)$ and 0.23 eV for $C_{169}Pt(c)$).[22]

2.4. Pt-Doped SWCNT Rods with Hydrogen Caps

With the shorter $C_{69}H_{20}Pt$ segment (Fig. 15), geometry optimization yielded data in strong agreement with the wall-doped fullerene-capped $C_{169}Pt$ nanorod. The Pt–C distances are 1.94, 1.94, and 2.01 Å and a positive charge of 0.83 remains on the Pt center. The HOMO–LUMO gap, however, has increased to 0.74 eV. Regardless, a clear analogy between the MOs of this segment and the wall-doped $C_{169}Pt(w)$ can be easily seen (see Figs. 14 and 16).[23]

3. GAS ADSORPTION ONTO METAL-DOPED SWCNTs

3.1. Adsorption of Carbon Monoxide

We first examined the adsorption of CO onto a Pt-doped SWCNT,[23] a gas that plays a significant role both in discrete organometallic complexes[112, 114, 128] and metal surfaces.[91, 92] The possibility of C-end adsorption (giving a CO-adsorbed HSWCNT) and O-end adsorption (giving an OC-adsorbed HSWCNT) were both considered (Fig. 17).[23]

The adsorption resulted in the release of 41.23 kcal mol^{-1} for C-end adsorption and 6.98 kcal mol^{-1} for O-end adsorption (Table I),[23] in agreement with classical coordination chemistry where the lone pair of electrons on the C atom donates into a metal *d*-orbital, causing a backdonation to the π^*-orbital of the adsorbate. The optimized geometry of the CO-adsorbed HSWCNT revealed a slight lengthening of the C≡O triple bond from 1.18 Å in the

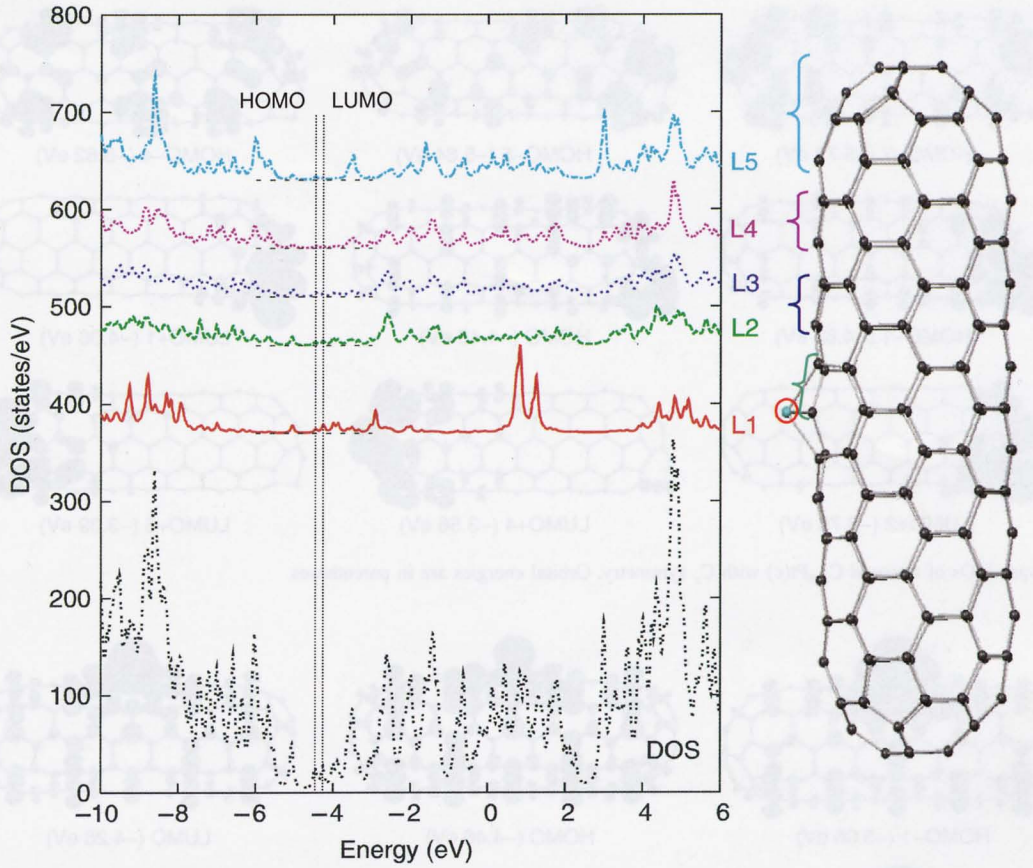

Fig. 11. Optimized geometry, DOS, and LDOS of $C_{169}Pt(w)$ with C_s symmetry ($\varepsilon_{HOMO} = -4.46$ eV, $\varepsilon_{LUMO} = -4.26$ eV). L1–L5 are the LDOS for each specified layer of atoms as marked on the diagram.

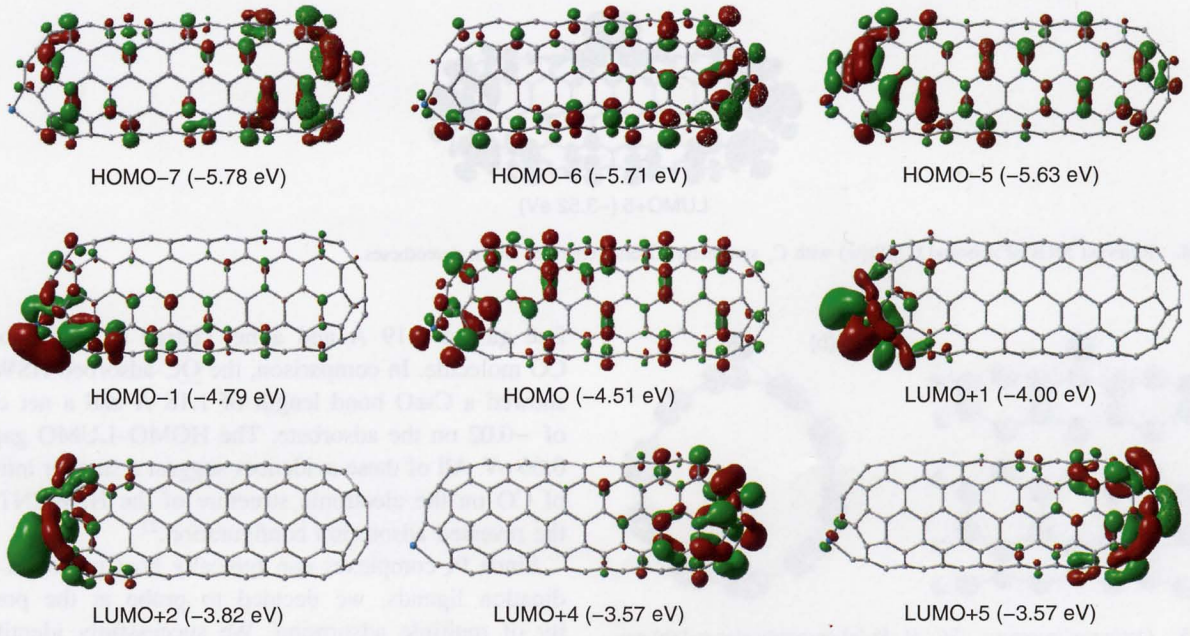

Fig. 12. Relevant MOs of nanorod $C_{169}Pt(ce)$ with C_s symmetry. Orbital energies are in parentheses.

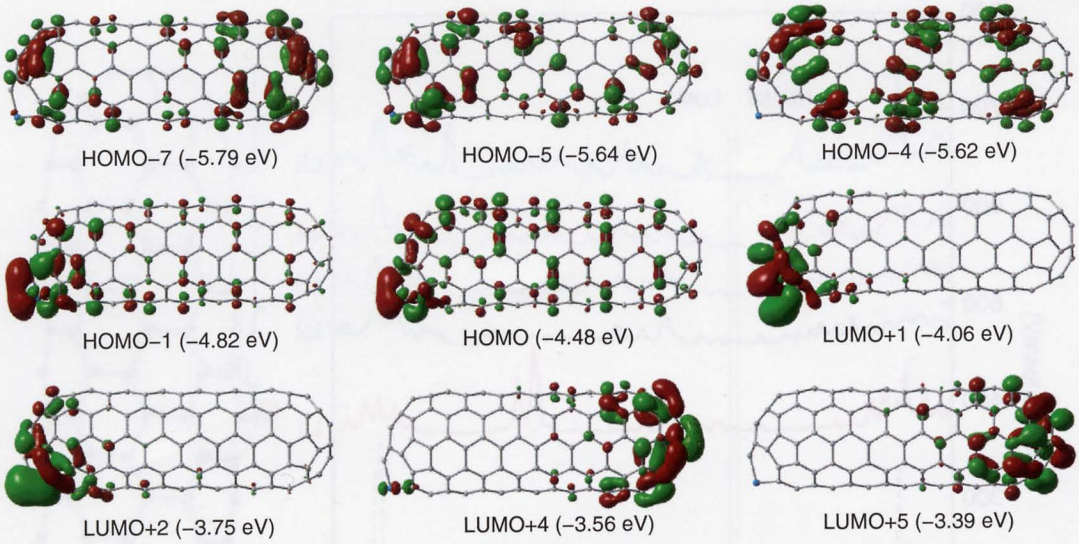

Fig. 13. Relevant MOs of nanorod $C_{169}Pt(c)$ with C_s symmetry. Orbital energies are in parentheses.

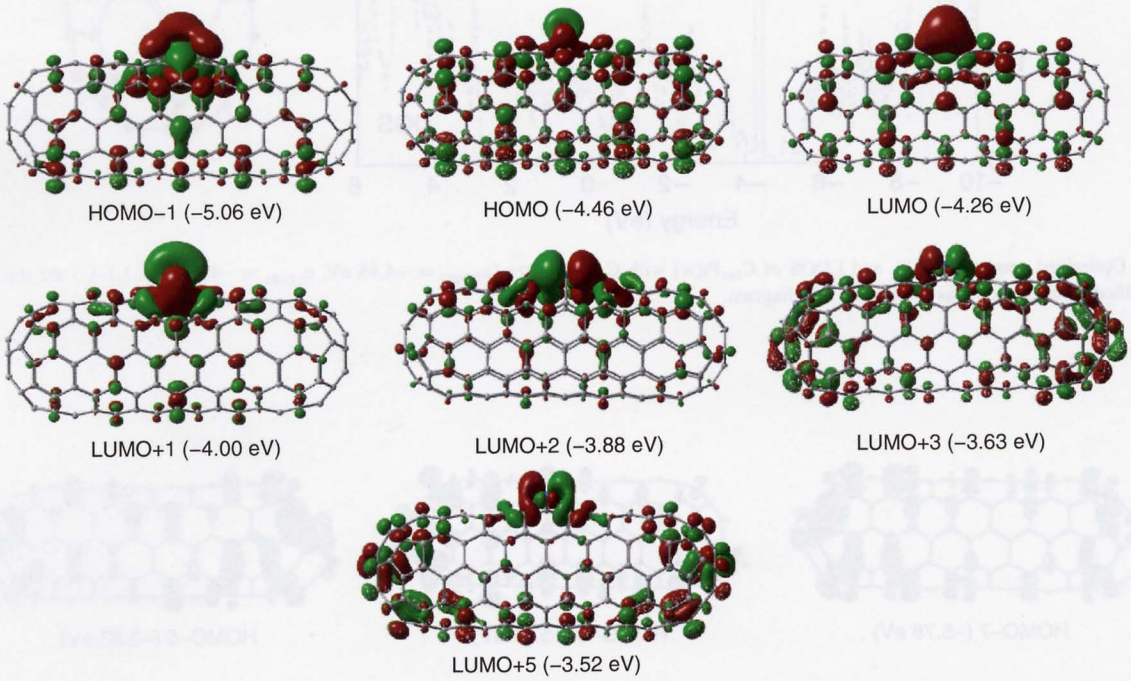

Fig. 14. Relevant MOs of nanorod $C_{169}Pt(w)$ with C_s symmetry. Orbital energies are in parentheses.

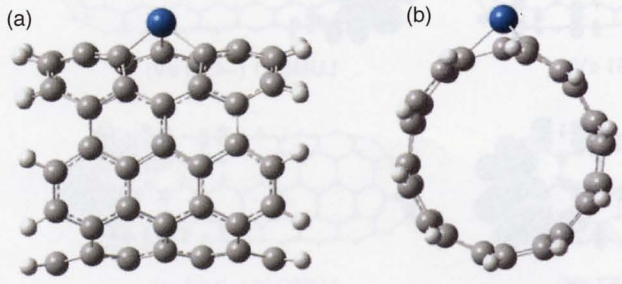

Fig. 15. Optimized geometry of $C_{69}H_{20}Pt$ (a) perpendicular and (b) parallel to the nanotube axis.

free gas to 1.19 Å and a net charge of −0.12 on the CO molecule. In comparison, the OC-adsorbed HSWCNT showed a C≡O bond length of 1.18 Å and a net charge of −0.02 on the adsorbate. The HOMO–LUMO gap was 0.66 eV. All of these evidences suggest a smaller influence of CO on the electronic structure of the HSWCNT with the reversed adsorption configuration.[23]

Since Pt complexes can typically host up to six coordination ligands, we decided to probe at the possibility of multiple adsorption. We successfully identified a structure with two molecules of CO attached to the Pt

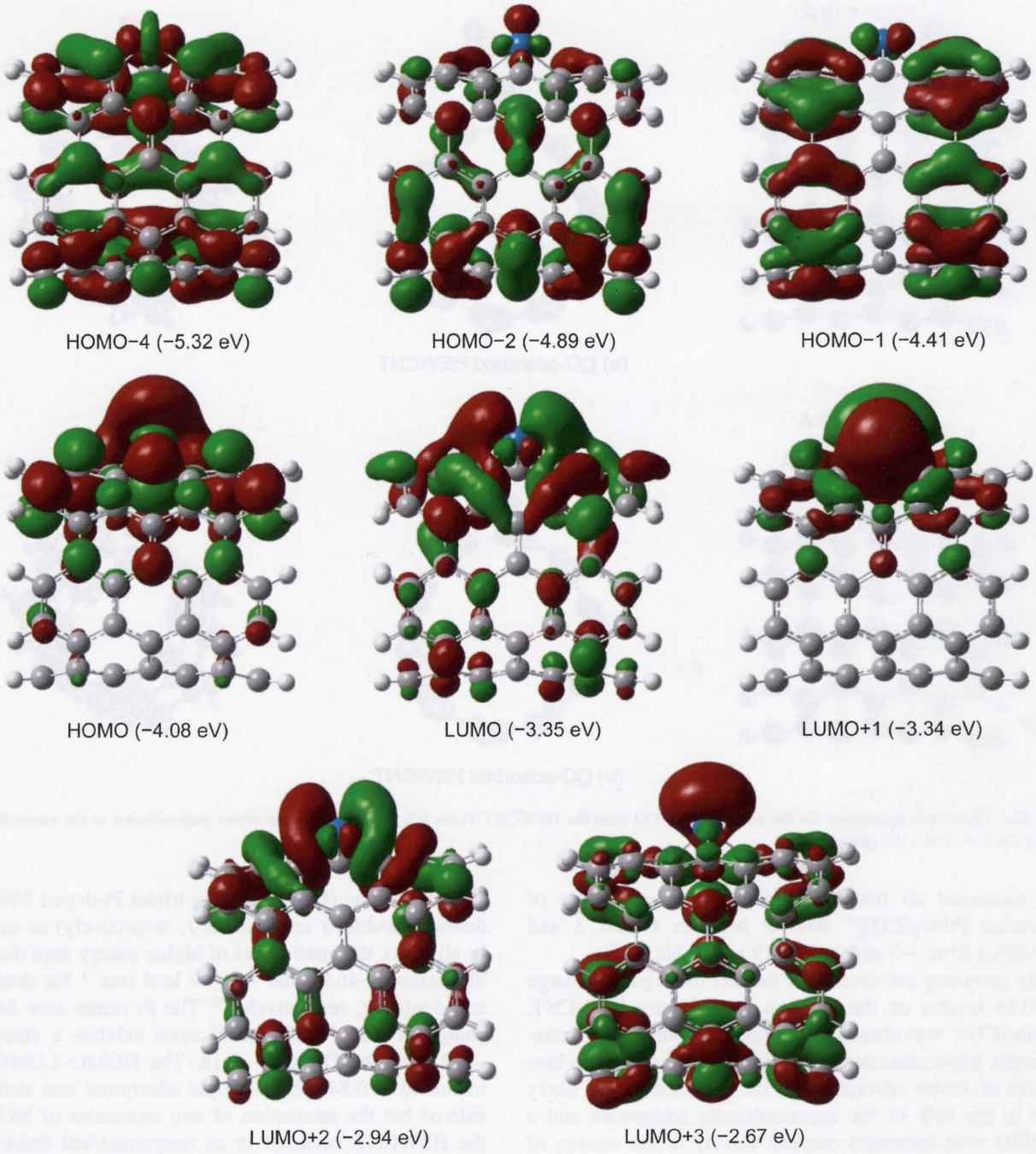

Fig. 16. Relevant MOs for ground state $C_{69}H_{20}Pt$. Orbital energies are in parentheses.

center through C-end adsorption (Fig. 18). The $(\underline{C}O)_2$-adsorbed HSWCNT segment was formed with a further release of energy (36.83 kcal mol^{-1}/molecule CO) and displayed almost identical orientation of both adsorbates, albeit with increased Pt–C distances (2.00 Å) and decreased net charges (−0.05/molecule CO).[23] For the case of triple adsorption, we could only locate a structure that was similar geometrically to the $(\underline{C}O)_2$-adsorbed HSWCNT but displayed a third molecule of CO interacting weakly with the nanotube itself (*cf.* 3.13 Å between the Pt and C atoms). The overall process is energetically downhill from the bare Pt-doped SWCNT but uphill from the doubly-adsorbed intermediate.[49]

3.2. Comparison with Alkylplatinum Complexes

In light of the ability of a HSWCNT to adsorb molecules of CO,[23] we investigated alkylplatinum complexes through DFT. Alkylplatinum complexes are well-precedented in the literature[129–131] but since our system was novel,

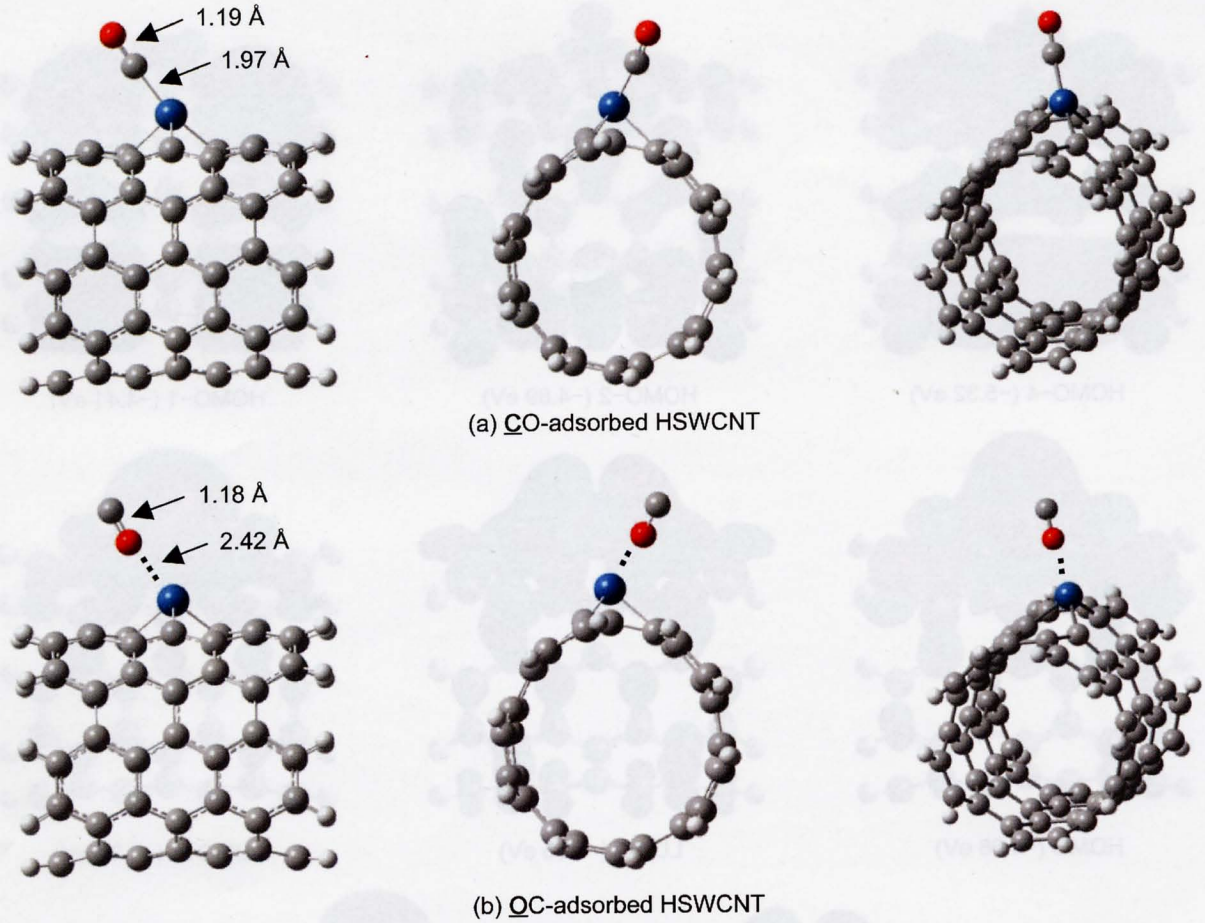

Fig. 17. Optimized geometries for the adsorption of CO onto the HSWCNT. From left to right, these are views perpendicular to the nanotube axis, along the axis, and a 3D perspective.

we examined all possible trimethylplatinum species of formulae $PtMe_3(CO)_x^{n+}$ with x between 0 and 3 and n ranging from −3 and 1 (Fig. 19 and Table II).[23]

By geometry and account of the fact that a partial charge of 0.83 resides on the Pt atom for the bare HSWCNT, $PtMe_3(CO)_x^+$ was chosen for comparison purposes.[23] Interestingly, triple adsorption *is* possible in this case. The limitation of double adsorption for the nanotube is thus likely due to the bulk of the supramolecular framework and a HOMO with decreased electron density in the vicinity of the Pt atom (Fig. 20).[23]

3.3. End-on Adsorption of Nitrogen-Based Gases: Nitrogen Monoxide, Ammonia, and Dinitrogen

We considered the adsorption of NO next (Fig. 18), which exists as a ground state doublet. The interaction between NO and Pt surfaces has been investigated,[132–135] but the use of this gas as a ligand is much less general (note that NO^+ and NO^- are both prevalent ligands in complexes). With the doublet state of the adsorbate, spin selection rules dictate that the resulting complex must have an electronic state of doublet (from singlet or triplet Pt-doped SWCNT, denoted doublet-*s* and doublet-*t*, respectively) or quartet. In all cases, the quartet was of higher energy than the doublet states (−46.97 and −56.49 kcal mol^{-1} for doublet-*s* and doublet-*t*, respectively).[49] The Pt center now bears a charge of 0.99, while the N atom exhibits a charge of −0.21 and the O atom −0.18. The HOMO–LUMO gap increased to 0.84 eV.[49] Multiple adsorption was also considered but the interaction of two molecules of NO with the HSWCNT occurred in an unsymmetrical fashion. In this case, one of the O atoms clearly points away from the nanotube (Fig. 21).[49] Adsorption of three NO molecules was not considered.

Another small molecule we investigated was NH_3, a common stabilizing ligand for a number of Pt complexes.[136–138] Heterogeneous Pt surfaces have also been shown to interact with this gas in the industrial oxidation of NH_3 to NO.[139] Unlike CO and NO, however, there is no low-lying π^*-orbital and backbonding is thus less likely to occur. The optimized geometry of a $\underline{N}H_3$-adsorbed HSWCNT $C_{69}H_{20}Pt(NH_3)$ revealed that the adsorption energy was −31.79 kcal mol^{-1} and the HOMO–LUMO gap was 0.73 eV. The interaction, however, appears to

Table I. Binding energy and geometrical data for nanotube-adsorbate complexes $C_{69}H_{20}Pt(XY)$ with end-on binding motif.

Adsorbate	Spin state	ΔE^a	$d(PtX)^b$	$d(XY)^c$	$q(Pt)^d$	$q(XY)^e$	$q(C)^f$
None[g]	Singlet	0			0.82		−0.41
	Triplet	0			0.84		−0.49
$\underline{C}O^{g,h}$	Singlet	−41.23	1.97	1.19	0.85	−0.12	−0.43
	Triplet	−33.09	1.96	1.20	0.83	−0.15	−0.46
$\underline{O}C^{g,h}$	Singlet	−6.98	2.42	1.18	0.87	−0.02	−0.41
	Triplet	−6.78	2.35	1.19	0.88	−0.06	−0.45
$(\underline{C}O)_2^{g,h}$	Singlet	−73.67	2.00, 2.00	1.19, 1.19	0.83	−0.05, −0.05	−0.49
	Triplet	−58.95	2.00, 2.00	1.19, 1.19	0.78	−0.02, −0.02	−0.49
$(\underline{C}O)_3^h$	Singlet	−71.35	1.98, 2.00, 3.13	1.19, 1.19, 1.19	0.77	0.01, −0.01, −0.06	−0.37
	Triplet	−73.74	2.03, 2.03, 2.41	1.18, 1.18, 1.19	0.76	0.05, 0.05, −0.13	−0.46
$\underline{N}O^h$	Doublet-*s*	−46.97	1.91	1.24	0.99	−0.39	−0.39
	Doublet-*t*	−56.49	1.91	1.24	0.99	−0.39	−0.39
	Quartet	−46.17	2.00	1.25	0.95	−0.38	−0.34
$\underline{O}N^h$	Doublet-*s*	−23.18	2.14	1.27	0.98	−0.37	−0.34
	Doublet-*t*	−32.71	2.14	1.27	0.98	−0.37	−0.34
	Quartet	−29.99	2.12	1.29	1.00	−0.44	−0.33
$(\underline{N}O)_2^h$	Singlet	−69.94	2.10, 2.12	1.24, 1.24	0.99	−0.24, −0.28	−0.36
	Triplet	−77.75	2.12, 2.12	1.24, 1.24	0.99	−0.25, −0.25	−0.35
$\underline{N}H_3^i$	Singlet	−31.79	2.25	N/A	0.88	0.18	−0.44
	Triplet	−31.28	2.23	N/A	0.87	0.18	−0.50
$(\underline{N}H_3)_2^i$	Singlet	−57.10	2.27, 2.27	N/A	0.92	0.18, 0.18	−0.48
	Triplet	−55.30	2.26, 2.26	N/A	0.86	0.19, 0.19	−0.49
N_2^i	Singlet	−24.72	2.08	1.16	0.91	−0.14	−0.41
	Triplet	−25.90	2.05	1.16	0.91	−0.18	−0.44
$(N_2)_2^i$	Singlet	−43.91	2.16, 2.16	1.16, 1.16	0.93	−0.09, −0.09	−0.42
	Triplet	−41.68	2.16, 2.16	1.16, 1.16	0.89	−0.09, −0.09	−0.41

[a]Total stabilization energy (in kcal mol^{-1}). [b]Distance (in Å) between Pt and X of XY. [c]Distance (in Å) between X and Y of XY. [d]Partial charge on Pt. [e]Net partial charge on XY. [f]Net partial charge on the C atoms of the SWCNT adjacent to Pt. [g]Ref. [20]. [h]$(\underline{X}Y)_n$ refers to an *n* X-end adsorbed HSWCNT fragment. [i]End-on adsorption.

be weaker since the distance from Pt to N was 2.25 Å (Fig. 18). We also found that the charge on the N atom was −1.13 and approximately 0.44 was present for each of the H atoms in NH_3. Thus, a net σ-donation appears to be occurring from the adsorbate to the SWCNT.[49] Two molecules of NH_3 were also shown to effectively adsorb onto the Pt center of this macromolecule with an energy change of −57.10 kcal mol^{-1}. In agreement with the observation for $(\underline{C}O)_2$-adsorbed HSWCNTs, the energy released per molecule decreased likely due to an increased steric effect between the two adsorbates.[49]

We then turned our attention to adsorbates that have no inherent polarity because these may also be important as analytes. N_2, in particular, has been the focus of much attention due to its role in the industrial fixation of nitrogen via the Haber-Bosch process. Interaction of a transition metal with N_2 can take place either through an end-on fashion with the N atom acting as a σ-donor to the metal, which typically requires the metal to be low-valent.[140] Side-on binding is also possible.[141] To our surprise, the structures of both end-on- and side-on-bound N_2 converged to give a geometry with an end-on-binding motif with the seventy-atom fragment ($C_{69}H_{20}Pt$). The energy that was released upon this adsorption was much less than CO adsorption (−24.72 kcal mol^{-1}), not unexpected because of the nonpolar character of the adsorbate. The observed N≡N distance was lengthened only slightly from 1.15 Å in the free gas to 1.16 Å in this complex (Fig. 18). Interestingly, the net charge on the N_2 molecule was −0.14, signifying a net donation of electrons from the Pt center to the oncoming ligand.[49] We were also able to identify a doubly adsorbed complex as in the case of CO and NO. In this scenario, though, the energy released per molecule of N_2 (−21.96 kcal mol^{-1}) was much closer to that of single adsorption (−24.72 kcal mol^{-1}). One possible explanation for this observation is that the weaker interaction between Pt and the adsorbate results in a smaller steric repulsion between the two N_2 molecules. The calculated HOMO–LUMO gap for this complex was 0.81 eV.[95]

3.4. Adsorption of Hydrogen Gas

From the above studies, it is clear that the incorporation of Pt into the sidewall of the SWCNT allows unique interactions with gases that are otherwise not possible. We then decided to examine the possibility of side-on adsorption, first examining the interaction of the HSWCNT with H_2 (Fig. 22 and Table III). Indeed, the activation of H_2 with Pt has found tremendous application in organic synthesis in regards to the hydrogenation of alkenes and alkynes. Our Pt-doped SWCNT is unique in the sense that it sits

REVIEW

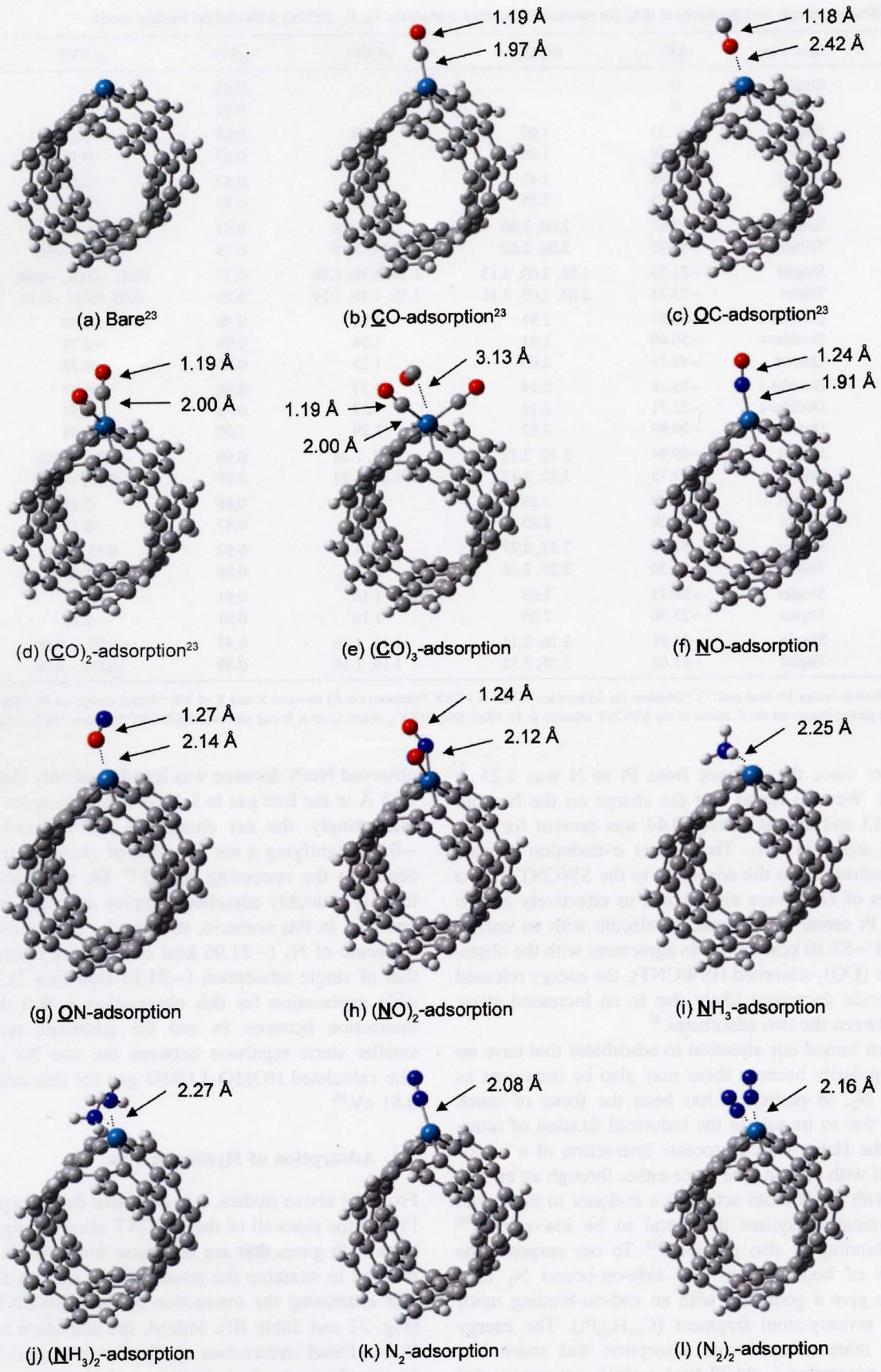

Fig. 18. Optimized geometries for end-on adsorbed HSWCNTs.

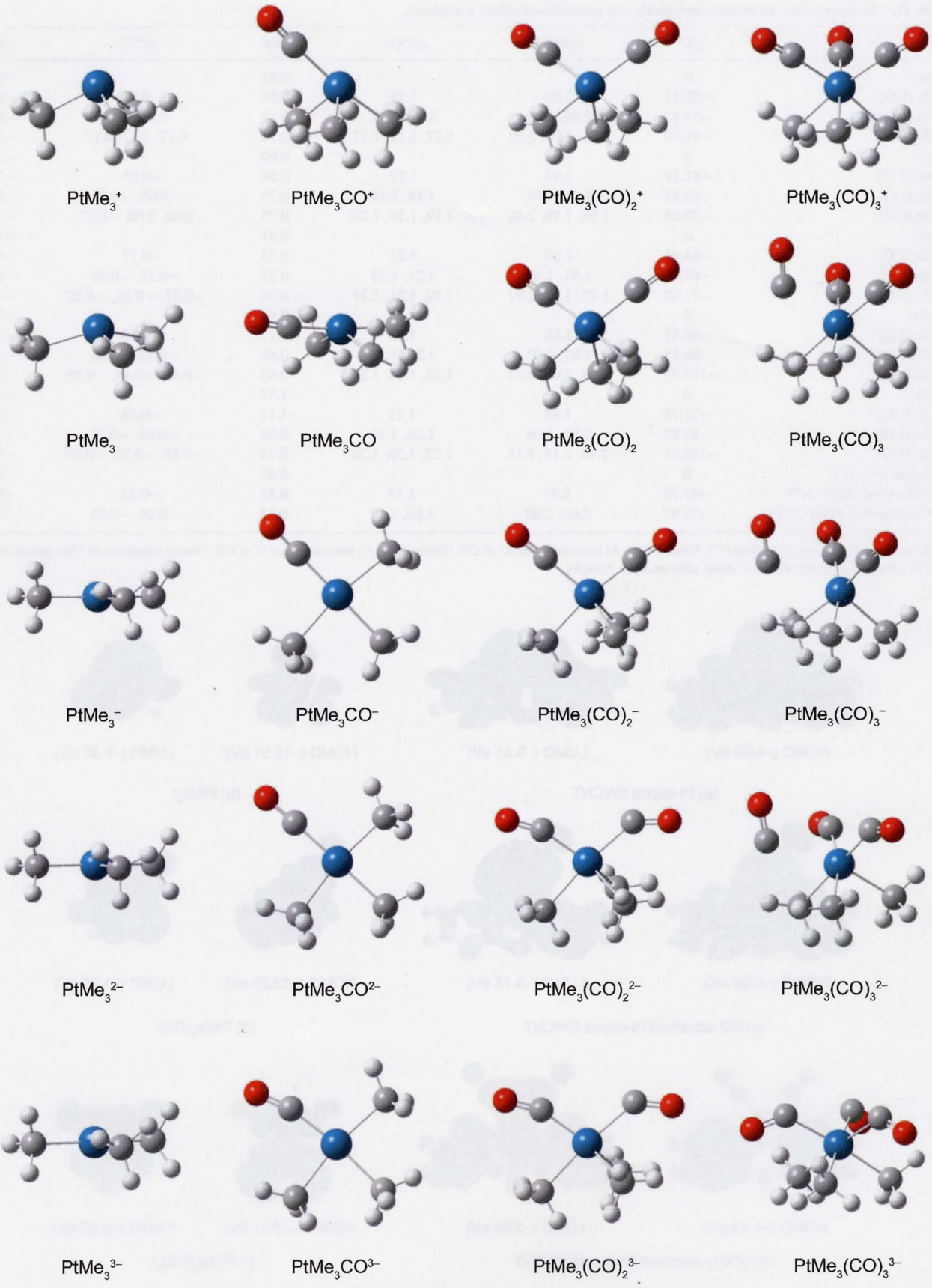

Fig. 19. Optimized geometries of alkylplatinum model compounds.

Table II. Summary data for model compounds and nanotube-adsorbate complexes.

Species	ΔE^a	d(PtC)^b	d(CO)^c	q(Pt)^d	q(CO)^e	q(C)^f
$PtMe_3^+$	0			0.83		−2.13
$PtMe_3(CO)^+$	−28.11	2.04	1.17	0.84	0.09	−2.22
$PtMe_3(CO)_2^+$	−55.41	2.05, 2.05	1.17, 1.17	0.79	0.14, 0.14	−2.34
$PtMe_3(CO)_3^+$	−81.90	2.05, 2.05, 2.05	1.17, 1.17, 1.17	0.74	0.17, 0.17, 0.17	−2.47
$PtMe_3$	0			0.60		−2.63
$PtMe_3(CO)$	−41.19	1.93	1.19	0.68	−0.05	−2.71
$PtMe_3(CO)_2$	−63.47	1.96, 1.96	1.19, 1.19	0.75	−0.05, −0.05	−2.70
$PtMe_3(CO)_3$	−70.64	1.98, 1.98, 2.40	1.19, 1.19, 1.20	0.75	0.00, 0.00, −0.17	−2.65
$PtMe_3^-$	0			0.31		−3.01
$PtMe_3(CO)^-$	−64.41	1.87	1.21	0.53	−0.17	−3.18
$PtMe_3(CO)_2^-$	−67.27	1.91, 1.92	1.21, 1.22	0.77	−0.25, −0.35	−3.03
$PtMe_3(CO)_3^-$	−77.30	1.92, 1.93, 2.97	1.20, 1.21, 1.21	0.76	−0.27, −0.22, −0.22	−2.94
$PtMe_3^{2-}$	0			−0.48		−3.10
$PtMe_3(CO)^{2-}$	−66.81	1.88	1.23	−0.15	−0.40	−3.20
$PtMe_3(CO)_2^{2-}$	−86.15	1.91, 2.03	1.25, 1.25	0.65	−0.55, −0.56	−3.24
$PtMe_3(CO)_3^{2-}$	−107.55	1.98, 2.00, 2.72	1.23, 1.24, 1.24	0.65	−0.43, −0.44, −0.45	−3.11
$PtMe_3^{3-}$	0			−1.57		−3.02
$PtMe_3(CO)^{3-}$	−71.74	1.88	1.23	−1.12	−0.38	−3.19
$PtMe_3(CO)_2^{3-}$	−93.82	1.91, 2.08	1.26, 1.26	0.08	−0.60, −0.73	−3.36
$PtMe_3(CO)_3^{3-}$	−130.61	2.14, 2.15, 2.15	1.25, 1.26, 1.26	0.21	−0.55, −0.55, −0.55	−3.25
Pt-doped SWCNT^g	0			0.82		−0.41
CO-adsorbed HSWCNT^g	−41.23	1.97	1.19	0.85	−0.12	−0.43
$(CO)_2$-adsorbed HSWCNT^g	−73.67	2.00, 2.00	1.19, 1.19	0.83	−0.05, −0.05	−0.49

^{a}Total stabilization energy (in kcal mol^{-1}). ^{b}Distance (in Å) between Pt and C of CO. ^{c}Distance (in Å) between C and O of CO. ^{d}Partial charge on Pt. ^{e}Net partial charge on CO. ^{f}Net partial charge on the C atoms adjacent to Pt. ^{g}Singlet.

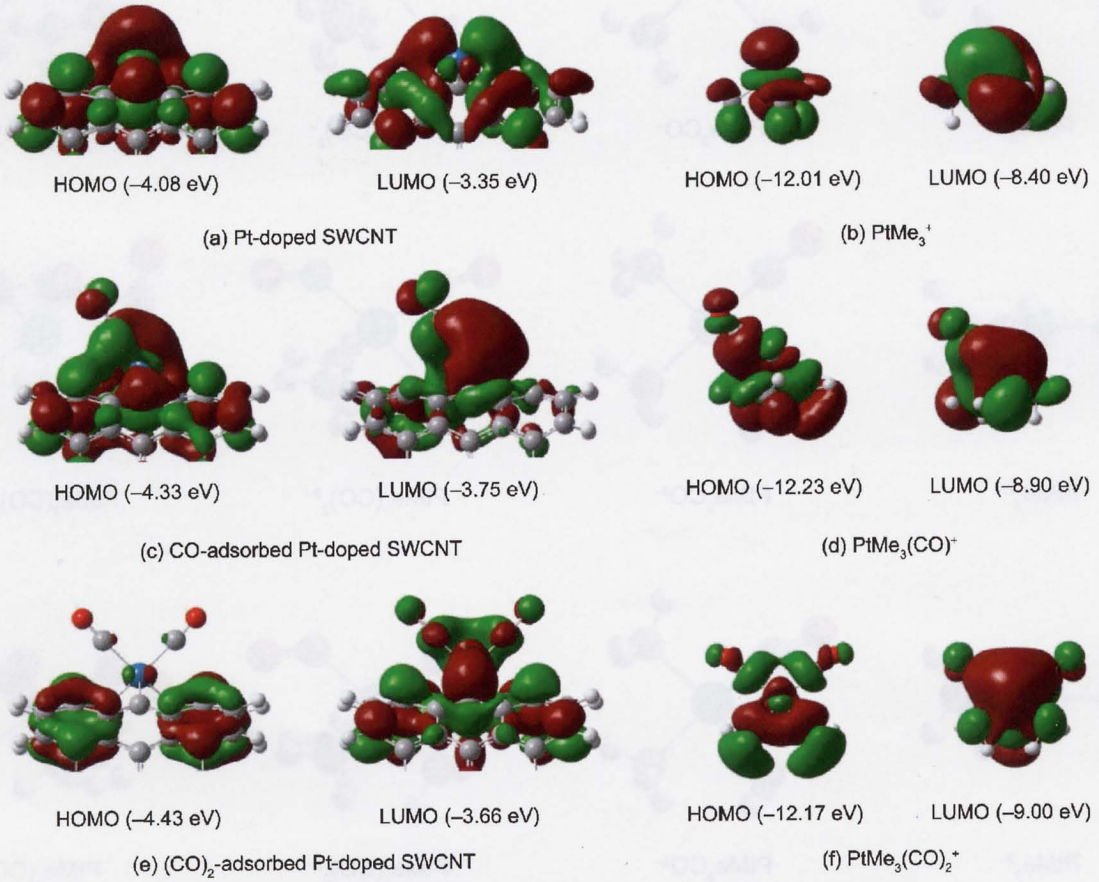

Fig. 20. Frontier MOs for the alkylplatinum complexes and Pt-doped SWCNT. Orbital energies are in parentheses.

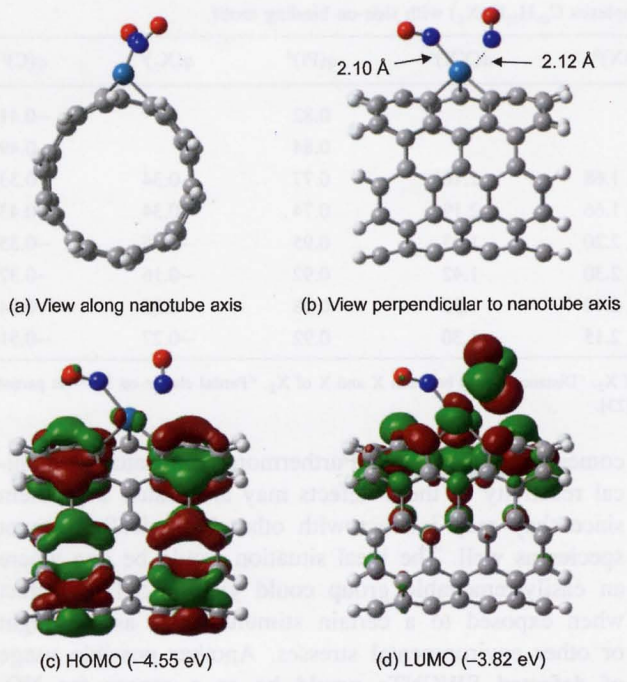

Fig. 21. $(NO)_2$-adsorbed HSWCNT. Orbital energies are in parentheses.

between the two extremes of heterogeneous and homogeneous activation of small molecules

The larger $C_{169}Pt$ nanorods were examined initially.[22] Interestingly, the location of the Pt atom had a drastic effect of the adsorption of H_2. In the case of both cap-doped HSWCNTs, the net process appeared to be physisorption with a relatively weak interaction between the Pt atom and the adsorbate. Only approximately 2.0 kcal mol^{-1} of energy was released in these cases, yielding geometries where the H–H distance was not significantly altered from that of free H_2. However, $C_{169}Pt(w)$ was found to interact strongly with H_2 and result in chemisorption and a formal oxidative addition taking place. The energy released for this process was close to 10.0 kcal mol^{-1}, almost five times that of the physisorption on the cap-doped HSWCNTs. Here, the distance between the H atoms has increased to 1.70 Å.[22]

In comparison, the smaller fragment $C_{69}H_{20}Pt$ also yielded a geometry similar to that observed for $C_{169}Pt(w)$ and resulted in the chemisorption of H_2 (*ca.* 2.16 Å separation between the two H atoms). The energetic preference for this reaction was −11.32 kcal mol^{-1} for the ground state. In this case, the HOMO–LUMO gap was 0.70 eV with a charge of 0.77 on the Pt atom and −0.34 on the adsorbate.[49]

3.5. Adsorption of Ethylene

The hydrogenation of alkenes and alkynes using transition metals as an activator also typically requires an interaction of the substrate with the surface. The simplest two-carbon alkene is ethylene (C_2H_4) and has been studied in regards to the difference between physisorption and chemisorption.[142]

With the larger Pt-doped nanorods, physisorption was observed to occur with Pt–C distances of approximately 2.30 Å. The strength of interaction as gauged by the length of the C=C bond seems to suggest a weaker adsorption at the caps (1.40 Å for $C_{169}Pt(ce)$, 1.41 Å for $C_{169}Pt(c)$) than the sidewall (1.42 Å for $C_{169}Pt(w)$) but clearly shows the effect of the transition metal (*cf.* 1.35 Å for the free gas). A close analysis of the energy changes associated with the physisorption process reveals that $C_{169}Pt(w)$ has the strongest interaction with C_2H_4.[22] These distances are in agreement with those reported for the adsorption of ethylene onto an Ir-doped fullerene.[143]

We confirmed that a molecule of C_2H_4 can also interact with the Pt center of $C_{69}H_{20}Pt$. The amount of energy released, however, was only −26.43 kcal mol^{-1} for the singlet electronic state (the HOMO–LUMO gap increased to 0.88 eV). The C=C distance was 1.43 Å in this case

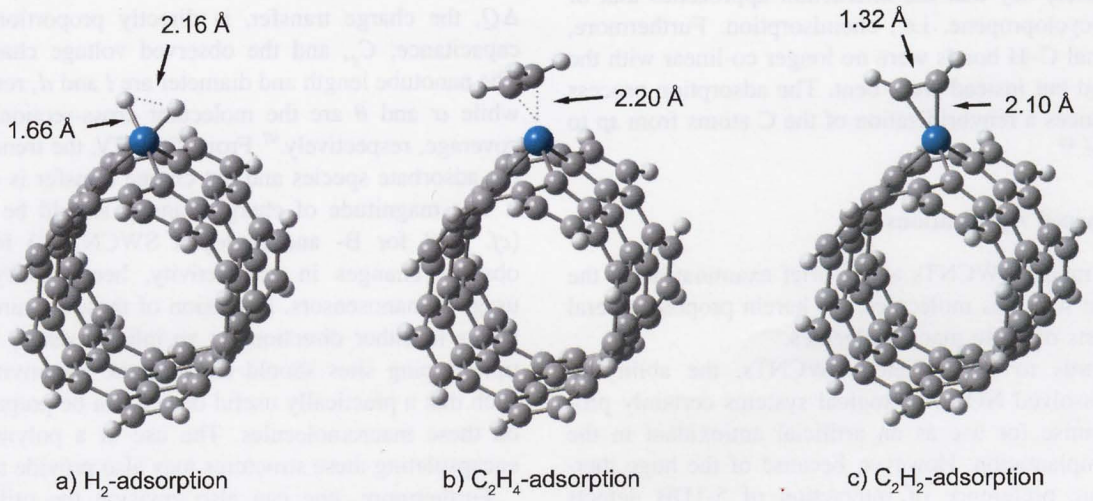

Fig. 22. Optimized geometries for side-on adsorbed HSWCNTs.

Table III. Binding energy and geometrical data for nanotube-adsorbate complexes $C_{69}H_{20}Pt(X_2)$ with side-on binding motif.

Adsorbate	X	Spin state	ΔE^a	$d(PtX)^b$	$d(XX)^c$	$q(Pt)^d$	$q(X_2)^e$	$q(C)^f$
None[g]		Singlet	0			0.82		−0.41
		Triplet	0			0.84		−0.49
H_2	H	Singlet	−11.32	1.66, 1.68	2.16	0.77	−0.34	−0.33
		Triplet	−6.02	1.66, 1.66	2.19	0.74	−0.34	−0.43
C_2H_4	CH_2	Singlet	−26.43	2.31, 2.20	1.43	0.95	−0.25	−0.35
		Triplet	−24.74	2.31, 2.30	1.42	0.92	−0.16	−0.37
C_2H_2	CH	Singlet	−31.36	2.13, 2.10	1.32	0.98	−0.38	−0.34
		Triplet	−25.29	2.17, 2.15	1.30	0.92	−0.27	−0.31

[a]Total stabilization energy (in kcal mol^{-1}). [b]Distances (in Å) between Pt and each X of X_2. [c]Distance (in Å) between X and X of X_2. [d]Partial charge on Pt. [e]Net partial charge on X_2. [f]Net partial charge on the C atoms of the SWCNT adjacent to Pt. [g]Ref. [23].

(Fig. 22 and Table III). A net charge of −0.25 on the adsorbate was found by NBO analysis.[49]

3.6. Adsorption of Acetylene

Having completed the investigation of the adsorption of ethylene, we turned to acetylene (C_2H_2), a small gas molecule that plays a significant role in the chemical industry.[95, 115] In fact, the utilization of a Pt surface for hydrogenation often results in the direct production of ethane.[95, 144, 145] Alkynes have also been shown to interact with transition metals both through weak donations of π-electrons of the adsorbate to the metal and more profound interactions that result in the oxidative addition of the transition metal, giving a metallocyclopropene.

With the smaller H-terminated SWCNT fragments, we found that the adsorption of C_2H_2 resulted in the liberation of 31.36 kcal mol^{-1} for the ground state configuration and lengthened the C≡C distance from 1.23 Å in the free gas to 1.32 Å (Fig. 22 and Table III). The HOMO–LUMO gap in this case was similar to that of ethylene at 0.88 eV and a net charge of −0.38 was found on the adsorbate (the Pt center bore a charge of 0.98). The separation between the Pt atom and either C atom was approximately 2.15 Å and we can safely say that the interaction approaches that of a metallocyclopropene, i.e., chemisorption. Furthermore, the terminal C–H bonds were no longer co-linear with the C≡C bond but instead were bent. The adsorption process hence induces a rehybridization of the C atoms from *sp* to almost sp^2.[49]

3.7. Proposed Applications

With the model SWCNTs and a brief examination of the interaction with gas molecules, we herein propose several applications of these macromolecules.

In regards to the defected SWCNTs, the ability to adsorb dissolved NO in biological systems certainly provides promise for use as an artificial antioxidant in the case of implantation. However, because of the huge thermodynamic preference of interaction of 5-1DB defects with this small molecule, the reversibility of the process comes into question.[50] Furthermore, the natural chemical reactivity of these defects may also cause a problem since they may interact with other biologically-relevant species as well. The ideal situation would be one where an easily-removable group could yield a 5-1DB defect when exposed to a certain stimulus such as UV light or other environmental stresses. Another possible usage of defected SWCNTs would be as a sensor for NO, specifically biological NO.[146] A more appropriate starting point for the development of a sensor, however, would be transition metal-doped SWCNTs. HSWCNTs could find potential utility in sensory technology and nanoelectronics, both utilizing the change in electronic structure due to adsorption. This effect, in theory, can be evaluated by the charge transfer from the macromolecule to the small molecule[97] and also by the HOMO–LUMO gap of the system.[23]

Peng and co-workers suggested that the charge transfer between the nanotube and adsorbate can result in a change in the conductance along the axis as described by the following relationship:[97]

$$\Delta Q = C_g \cdot \Delta V_g = \delta\theta \frac{\pi dl}{\sigma} \quad (1)$$

ΔQ, the charge transfer, is directly proportional to the capacitance, C_g, and the observed voltage change, ΔV_g. The nanotube length and diameter are l and d, respectively, while σ and θ are the molecular cross-section area and coverage, respectively.[97] From Table IV, the trend between the adsorbate species and net charge transfer is clear.[49]

The magnitude of charge transfer should be sufficient (*cf.* 0.28 for B- and N-doped SWCNTs[97]) for one to observe changes in conductivity, hence ratifying their usage as nanosensors. Extension of these terminated fragments in either direction (in an infinite sense) with multiple doping sites should enhance the sensitivity enough such that a practically useful device can be prepared based on these macromolecules. The use of a polymer matrix encapsulating these structures may also provide some help.

Furthermore, one can also envision the utilization of these macromolecules as nanowires. In the developing

Table IV. Charge transfer and HOMO–LUMO gap (in eV) data for nanotube-adsorbate complexes with side-on binding motif.

Analyte	Average charge transfer[a]	HOMO–LUMO gap
None[b]		0.74
CO[c]	0.05	0.78
NO[d]	0.28	0.74
NH_3[e]	−0.18	0.75
N_2[f]	0.09	0.81
H_2	0.34	0.70
C_2H_2	0.38	0.88
C_2H_4	0.25	0.88

[a]Represents charge donated from the Pt-doped SWCNT to the adsorbate. [b]Ref. [23]. [c]Represents $(\underline{C}O)_2$-adsorbed HSWCNT. [d]Represents $(\underline{N}O)_2$-adsorbed HSWCNT. [e]Represents $(\underline{N}H_3)_2$-adsorbed HSWCNT. [f]Represents $(N_2)_2$-adsorbed HSWCNT.

field of nanoelectronics, the ability of manipulating conductance across a wire with simple exposure to gases is an attractive one since this would allow for strict control of a nanocircuit. Obviously, the selective modification of one SWCNT in the presence of thousands of others would still be a challenge and may require new engineering solutions, but the potential of doing this in a reversible fashion is indeed intriguing because one could easily imagine an operation where the presence of certain types of gases can break a circuit and trigger an electrical response.

4. CONCLUDING REMARKS

Within DFT, defected and doped SWCNTs indeed have a rich chemistry. We summarize our findings below:

1. A 5-1DB defect results in the protrusion of a single active C atom that can interact with NO to give NO_2 and a N-doped SWCNT in a selective manner.
2. Pt-doped SWCNTs display geometries where the Pt tends to be situated in a position outside of the sidewall, likely due to its large size.
3. Cap-doped HSWCNTs display different electronic structures and reactivity in comparison to wall-doped species. The interaction between metal atoms and small gas molecules is typically stronger along the sidewall, likely due to a higher concentration of electron density around the Pt center and hence the ability for donation/backdonation.
4. The adsorption of linear molecules takes place in analogy to alkylplatinum complexes in the Pt(IV) oxidation state. However, the steric bulk of the nanotube as a supramolecular ligand may prevent the possibility of multiple adsorption. In these cases, interaction with the nanotube π-electrons themselves may be possible.

Without a doubt, since transition metal-doped SWCNTs have yet to be prepared experimentally, much of the work presented here remains to be theoretical prediction. Nonetheless, we have provided a comprehensive overview on the electronic properties of these materials. Their behavior in polymer composites, in particular, may provide a handle by which some of these properties can be amplified to useful levels. Further studies in this field such as examination of segments with periodic boundary conditions will provide a closer look at the vast usage of these novel materials. We hope that our initial investigations will provide inspiration and guidance to experimentalists in their endeavors.

Acknowledgments: We thank the Natural Sciences and Engineering Research Council (NSERC) of Canada for financial support. WestGrid and C-HORSE have provided the necessary computational resources. Charles See Yeung gratefully acknowledges NSERC for an Undergraduate Student Research Award. Lei Vincent Liu thanks the University of British Columbia for Gladys Estella Laird and Charles A. McDowell fellowships.

References

1. S. Iijima, *Nature* 354, 56 (**1991**).
2. S. Iijima and T. Ichihashi, *Nature* 363, 603 (**1993**).
3. D. Tasis, N. Tagmatarchis, A. Bianco, and M. Prato, *Chem. Rev.* 106, 1105 (**2006**).
4. P. M. Ajayan, *Chem. Rev.* 99, 1787 (**1999**).
5. H. R. Byon and H. C. Choi, *J. Am. Chem. Soc.* 128, 2188 (**2006**).
6. N. Ferrer-Anglada, V. Gomis, Z. El-Hachemi, U. D. Weglikovska, M. Kaempgen, and S. Roth, *Phys. Stat. Solid.* 203, 1082 (**2006**).
7. P. Avouris, *Acc. Chem. Res.* 35, 1026 (**2002**).
8. Z. Chen, J. Appenzeller, Y.-M. Lin, J. Sippel-Oakley, A. G. Rinzler, J. Tang, S. J. Wind, P. M. Solomon, and P. Avouris, *Science* 311, 1735 (**2006**).
9. N. Robertson and C. A. McGowan, *Chem. Soc. Rev.* 32, 96 (**2003**).
10. D. A. Britz and A. N. Khlobystov, *Chem. Soc. Rev.* 35, 637 (**2006**).
11. Y. Yeo-Heung, A. Miskin, P. Kang, S. Jain, S. Narasimhadevara, D. Hurd, V. Shinde, M. J. Schulz, V. Shanov, P. He, F. J. Boerio, D. Shi, and S. Srivinas, *J. Intel. Mater. Sys. Struc.* 17, 107 (**2006**).
12. M. Nakazawa, S. Nakahara, T. Hirooka, M. Yoshida, T. Kaino, and K. Komatsu, *Opt. Lett.* 31, 915 (**2006**).
13. S. Y. Set, H. Yaguchi, Y. Tanaka, and M. Jablonski, *J. Lightwave Technol.* 22, 51 (**2004**).
14. D. H. Wu, W. T. Chien, C. S. Chen, and H. H. Chen, *Sens. Act. A* 126, 117 (**2006**).
15. J. Kim, J. Baek, H. Kim, K. Lee, and S. Lee, *Sens. Act. A* 128, 7 (**2006**).
16. M. E. Kose, B. A. Harruff, Y. Lin, L. M. Veca, F. Lu, and Y.-P. Sun, *J. Phys. Chem. B* 110, 14032 (**2006**).
17. W. Wongwiriyapan, S.-I. Honda, H. Konishi, T. Mizuta, T. Ikuno, T. Ito, T. Maekawa, K. Suzuki, H. Ishikawa, K. Oura, and M. Katayama, *Jap. J. Appl. Phys.* 44, L482 (**2005**).
18. H. Zhang, *J. Nanoparticle Res.* 6, 665 (**2004**).
19. P. Serp, M. Corrias, and P. Kalck, *Appl. Catal. A* 253, 337 (**2003**).
20. M. Moniruzzaman and K. I. Winey, *Macromolecules* 39, 5194 (**2006**).
21. M. S. Dresselhaus, G. Dresselhaus, and P. C. Eklund, Science of Fullerenes and Carbon Nanotubes, Academic, San Diego (**1995**), Chap. 19.
22. W. Q. Tian, L. V. Liu, and Y. A. Wang, *Phys. Chem. Chem. Phys.* 8, 3528 (**2006**).
23. C. S. Yeung, L. V. Liu, and Y. A. Wang, *J. Comput. Theor. Nanosci.* 4, 1108 (**2007**).
24. M. B. Bryning, M. F. Islam, J. M. Kikkawa, and A. G. Yodh, *Adv. Mater.* 17, 1186 (**2005**).

25. F. Du, J. E. Fischer, and K. I. Winey, *Phys. Rev. B* 72, 121404 (**2005**).
26. M. Foygel, R. D. Morris, D. Anez, S. French, and V. L. Sobolev, *Phys. Rev. B* 71, 104201 (**2005**).
27. S. Barrau, P. Demont, E. Perez, A. Peigney, C. Laurent, and C. Lacabanne, *Macromolecules* 36, 9678 (**2003**).
28. F. Du, J. E. Fischer, and K. I. Winey, *J. Polym. Sci. B: Polym. Phys.* 41, 3333 (**2003**).
29. R. Haggenmueller, H. H. Gommans, A. G. Rinzler, J. E. Fischer, and K. I. Winey, *Chem. Phys. Lett.* 330, 219 (**2000**).
30. Q. Yuan and R. D. K. Misra, *Mater. Sci. Technol.* 22, 742 (**2006**).
31. V. I. Rodughin and V. V. Vysotskii, *Prog. Org. Coat.* 39, 81 (**2000**).
32. B. E. Kilbride, J. N. Coleman, J. Fraysse, P. Fournet, M. Cadek, A. Drury, S. Hutzler, S. Roth, and W. J. Blau, *J. Appl. Phys.* 92, 4024 (**2002**).
33. P. L. McEuen, M. Bockrath, D. H. Cobden, Y.-G. Yoon, and S. G. Louie, *Phys. Rev. Lett.* 83, 5098 (**1999**).
34. L. Valentini, I. Armentano, D. Puglia, and J. M. Kenny, *Carbon* 42, 323 (**2004**).
35. T. Ramanathan, H. Liu, and L. C. Brinson, *J. Polym. Sci. B: Polym. Phys.* 43, 2269 (**2005**).
36. E. Tamburri, S. Orlanducci, M. L. Terranova, F. Valentini, G. Pallesci, A. Curulli, F. Brunetti, D. Passeri, A. Alippi, and M. Rossi, *Carbon* 43, 1213 (**2005**).
37. P. J. Boul, J. Liu, E. T. Mickelson, C. B. Huffman, L. M. Ericson, I. W. Chiang, K. A. Smith, D. T. Colbert, R. H. Hauge, J. L. Margrave, and R. E. Smalley, *Chem. Phys. Lett.* 310, 367 (**1999**).
38. E. T. Mickelson, I. W. Chiang, J. L. Zimmermann, P. J. Boul, J. Lozano, J. Liu, R. E. Smalley, R. H. Hauge, and J. L. Margrave, *J. Phys. Chem. B* 103, 4318 (**1999**).
39. M. Holzinger, O. Vostrowsky, A. Hirsch, F. Hennrich, M. Kappes, R. Weiss, and F. Jellen, *Angew. Chem., Int. Ed.* 40, 2002 (**2001**).
40. V. Georgakilas, K. Kordatos, M. Prato, D. M. Guldi, M. Holzinger, and A. Hirsch, *J. Am. Chem. Soc.* 124, 760 (**2002**).
41. M. Holzinger, J. Abraham, P. Whelan, R. Graupner, L. Ley, F. Hennrich, M. Kappes, and A. Hirsch, *J. Am. Chem. Soc.* 125, 8566 (**2003**).
42. N. Tagmatarchis, V. Georgakilas, M. Prato, and H. Shinohara, *Chem. Commun.* 2010 (**2002**).
43. F. Liang, A. K. Sadana, A. Peera, J. Chattopadhyay, Z. Gu, R. H. Hauge, and W. E. Billups, *Nano Lett.* 4, 1257 (**2004**).
44. L. Long, X. Lu, F. Tian, and Q. Zhang, *J. Org. Chem.* 68, 4495 (**2003**).
45. D. Golberg, Y. Bando, W. Han, K. Kurashima, and T. Sato, *Chem. Phys. Lett.* 308, 337 (**1999**).
46. S. L. Sung, S. H. Tsai, C. H. Tseng, F. K. Chiang, X. W. Liu, and H. C. Shih, *Appl. Phys. Lett.* 74, 197 (**1999**).
47. P. L. Gai, O. Stephan, K. McGuire, A. M. Rao, M. S. Dresselhaus, G. Dresselhaus, and C. Colliex, *J. Mater. Chem.* 14, 669 (**2004**).
48. M. Glerup, J. Steinmetz, D. Samaille, O. Stephan, S. Enouz, A. Loiseau, S. Roth, and P. Bernier, *Chem. Phys. Lett.* 387, 193 (**2004**).
49. C. S. Yeung, L. V. Liu, and Y. A. Wang, *J. Phys. Chem. C* 112, 7401 (**2008**).
50. L. V. Liu, W. Q. Tian, and Y. A. Wang, *J. Phys. Chem. B* 110, 1999 (**2006**).
51. M. Terrones, A. Jorio, M. Endo, A. M. Rao, Y. A. Kim, T. Hayashi, H. Terrones, J.-C. Charlier, G. Dresselhaus, and M. S. Dresselhaus, *Mater. Today* 7, 30 (**2004**).
52. D. Srivastava, M. Menon, C. Daraio, S. Jin, B. Sadanadan, and A. M. Rao, *Phys. Rev. B* 69, 153414 (**2004**).
53. S. H. Yang, W. H. Shin, J. W. Lee, S. Y. Kim, S. I. Woo, and J. K. Kang, *J. Phys. Chem. B* 110, 13941 (**2006**).
54. S. Dag, Y. Ozturk, S. Ciraci, and T. Yildirim, *Phys. Rev. B* 72, 155404 (**2005**).
55. G. Mpourmpakis, G. E. Froudakis, A. N. Andriotis, and M. Menon, *Appl. Phys. Lett.* 87, 193105 (**2005**).
56. W.-Q. Deng, X. Lu, and W. A. Goddard III, *Nano Lett.* 4, 2331 (**2004**).
57. A. Thess, R. Lee, P. Nikolaev, H. Dai, P. Petit, J. Robert, C. Xu, Y. H. Lee, S. G. Kim, A. G. Rinzler, D. T. Colbert, G. E. Scuseria, D. Tománek, J. E. Fischer, and R. E. Smalley, *Science* 273, 483 (**1996**).
58. W. Branz, I. M. L. Billas, N. Malinowski, F. Tast, M. Heinebrodt, and T. P. Martin, *J. Chem. Phys.* 109, 3425 (**1998**).
59. J. M. Poblet, J. Munoz, K. Winkler, M. Cancilla, A. Hayashi, C. B. Lebrilla, and A. L. Balch, *Chem. Commun.* 6, 493 (**1999**).
60. Q. Kong, J. Zhuang, X. Li, R. Cai, L. Zhao, S. Qian, and Y. Li, *Appl. Phys. A* 75, 367 (**2002**).
61. C. Ding, J. Yang, X. Cui, and C. T. Chan, *J. Chem. Phys.* 111, 8481 (**1999**).
62. G. Lu, K. Deng, H. Wu, J. Yang, and X. Wang, *J. Chem. Phys.* 124, 054305 (**2006**).
63. W. Q. Tian, L. V. Liu, and Y. A. Wang, Handbook of Theoretical and Computational Nanotechnology, Vol. 9, edited by M. Rieth and W. Schommers, American Scientific, Valencia, California, USA (**2006**), Chap. 10, pp. 499–524.
64. W. Q. Tian, L. V. Liu, Y.-K. Chen, and Y. A. Wang, Trends in Computational Nanomechanics: Transcending Time and Space, edited by T. Dumitrica, Springer, Heidelberg (**2009**).
65. A. Nel, T. Xia, L. Mädler, and N. Li, *Science* 311, 622 (**2006**).
66. A. S. Karakoti, L. L. Hench, and S. Seal, *JOM* 58, 77 (**2006**).
67. R. F. Service, *Science* 304, 1732 (**2004**).
68. K. L. Dreher, *Toxicol. Sci.* 77, 3 (**2004**).
69. H. M. Kipen and D. L. Laskin, *Am. J. Physiol. Lung Cell. Mol. Physiol.* 289, L696 (**2005**).
70. K. Donaldson and C. L. Tran, *Inhal. Toxicol.* 14, 5 (**2002**).
71. A. Nel, *Science* 308, 804 (**2005**).
72. A. T. Bell, *Science* 299, 1688 (**2003**).
73. B. Halliwell and J. M. C. Gutteridge, Free Radicals in Biology and Medicine, Oxford University Press, Oxford (**1999**).
74. L. Ding, J. Stilwell, T. Zhang, O. Elboudwarej, H. Jiang, J. P. Selegue, P. A. Cooke, J. W. Gray, and F. F. Chen, *Nano Lett.* 5, 2448 (**2005**).
75. V. E. Kagan, Y. Y. Tyurina, V. A. Tyurin, N. V. Konduru, A. I. Potapovich, A. N. Osipov, E. R. Kisin, D. Schwegler-Berry, R. Mercer, V. Castranova, and A. A. Shvedova, *Toxicol. Lett.* 165, 88 (**2006**).
76. G. Jia, H. Wang, L. Yan, X. Wang, R. Pei, T. Yan, Y. Zhao, and X. Guo, *Environ. Sci. Technol.* 39, 1378 (**2005**).
77. J. Cheng, E. Flahaut, and S. H. Cheng, *Environ. Toxicol. Chem.* 26, 708 (**2007**).
78. N. N. Greenwood and A. Earnshaw, Chemistry of the Elements, 2nd edn., Butterworth-Heinemann, London (**1997**).
79. E. Culotta, E. Daniel, and J. Koshland, *Science* 258, 1862 (**1992**).
80. M. R. Miller and I. L. Megson, *Brit. J. Pharmacol.* 151, 305 (**2007**).
81. J. M. Fukuto and L. J. Ignarro, *Acc. Chem. Res.* 30, 149 (**1997**).
82. B. I. Jugdutt, *Heart Failure Rev.* 7, 385 (**2002**).
83. D. Bruch-Gerharz, T. Ruzicka, and V. Kolb-Bachofen, *J. Invest. Dermatol.* 110, 1 (**1998**).
84. R. P. Hunter, *Animal Health Res. Rev.* 3, 119 (**2002**).
85. R. L. Scher, *Laryngoscope* 117, 199 (**2007**).
86. O. W. Griffith and D. J. Stuehr, *Annu. Rev. Physiol.* 57, 707 (**1995**).
87. P. Vallance and J. Leiper, *Nature Rev. Drug Disc.* 1, 939 (**2002**).
88. P. S. Wheatley, A. R. Butler, M. S. Crane, S. Fox, B. Xiao, A. G. Rossi, I. L. Megson, and R. E. Morris, *J. Am. Chem. Soc.* 128, 502 (**2006**).
89. M. C. Frost, M. M. Reynolds, and M. E. Meyerhoff, *Biomaterials* 26, 1685 (**2005**).
90. E. B. Caruso, S. Petralia, S. Conoci, S. Giuffrida, and S. Sortino, *J. Am. Chem. Soc.* 129, 480 (**2007**).
91. H. Orita and Y. Inada, *J. Phys. Chem. B* 109, 22469 (**2005**).
92. H. Orita, N. Itoh, and Y. Inada, *Chem. Phys. Lett.* 384, 271 (**2004**).

93. P. Kaér, M. Kuzma, and L. Éervaný, *Appl. Catal. A* 259, 179 (**2004**).
94. J. Kong, M. G. Chapline, and H. Dai, *Adv. Mater.* 13, 1384 (**2001**).
95. F. J. Williams, A. Palermo, S. Tracey, M. S. Tikhov, and R. M. Lambert, *J. Phys. Chem. B* 106, 5668 (**2002**).
96. M. Lucci, A. Reale, A. D. Carlo, S. Orlanducci, E. Tamburri, M. L. Terranova, I. Davoli, C. D. Natale, A. D'Amico, and R. Paolesse, *Sens. Act. B* 118, 226 (**2006**).
97. S. Peng and K. Cho, *Nano Lett.* 3, 513 (**2003**).
98. E. Bekyarova, M. Davis, T. Burch, M. E. Itkis, B. Zhao, S. Sunshine, and R. C. Haddon, *J. Phys. Chem. B* 108, 19717 (**2004**).
99. P. G. Collins, K. Bradley, M. Ishigami, and A. Zettl, *Science* 287, 1801 (**2000**).
100. J. Kong, N. R. Franklin, C. W. Zhou, M. G. Chapline, S. Peng, K. J. Cho, and H. J. Dai, *Science* 287, 622 (**2000**).
101. L. B. da Silva, S. B. Fagan, and R. Mota, *Nano Lett.* 4, 65 (**2004**).
102. J. J. P. Stewart, *J. Comput. Chem.* 10, 209 (**1989**).
103. C. Lee, W. Yang, and R. G. Parr, *Phys. Rev. A* 37, 785 (**1988**).
104. A. D. Becke, *J. Chem. Phys.* 98, 5648 (**1993**).
105. B. Miehlich, A. Savin, H. Stoll, and H. Preuss, *Chem. Phys. Lett.* 157, 200 (**1989**).
106. R. Ditchfield, W. J. Hehre, and J. A. Pople, *J. Chem. Phys.* 54, 724 (**1971**).
107. W. J. Hehre, R. Ditchfield, and J. A. Pople, *J. Chem. Phys.* 56, 2257 (**1972**).
108. P. C. Hariharan and J. A. Pople, *Mol. Phys.* 27, 209 (**1974**).
109. M. S. Gordon, *Chem. Phys. Lett.* 76, 163 (**1980**).
110. F. Maseras and K. Morokuma, *J. Comput. Chem.* 16, 1170 (**1995**).
111. A. K. Rappe, C. J. Casewit, K. S. Colwell, W. A. Goddard III, and W. M. Skiff, *J. Am. Chem. Soc.* 114, 10024 (**2004**).
112. P. Mastrorilli, C. F. Nobile, G. P. Suranna, F. P. Fanizzi, G. Ciccarella, U. Englert, and Q. Li, *Eur. J. Inorg. Chem.* 1234 (**2004**).
113. A. W. Ehlers, S. Dapprich, S. F. Vyboishchikov, and G. Frenking, *Organometallics* 15, 105 (**1996**).
114. J. Puga, R. Patrini, K. M. Sanchez, and B. C. Gates, *Inorg. Chem.* 30, 2479 (**1991**).
115. J. W. Medlin and M. D. Allendorf, *J. Phys. Chem. B* 107, 217 (**2003**).
116. A. D. Becke, *Phys. Rev. A* 38, 3098 (**1988**).
117. J. P. Perdew, J. A. Chevary, S. H. Vosko, K. A. Jackson, M. R. Pederson, D. J. Singh, and C. Fiolhais, *Phys. Rev. B* 46, 6671 (**1992**).
118. J. P. Perdew, K. Burke, and Y. Wang, *Phys. Rev. B* 54, 16533 (**1996**).
119. P. J. Hay and W. R. Wadt, *J. Chem. Phys.* 82, 299 (**1985**).
120. J. P. Perdew, K. Burke, and M. Ernzerhof, *Phys. Rev. Lett.* 77, 3865 (**1996**).
121. E. D. Glendening, A. E. Carpenter, and F. Weinhold, *NBO*, Version 3.1 (**1995**).
122. A. E. Reed, L. A. Curtiss, and F. Weinhold, *Chem. Rev.* 88, 899 (**1988**).
123. A. Tenderholt, *PyMOlyze*, Version 1.1 (**2005**).
124. M. J. Frisch, G. W. Trucks, H. B. Schlegel, G. E. Scuseria, M. A. Robb, J. R. Cheeseman, J. A. Montgomery, T. Vreven, K. N. Kudin, J. C. Burant, J. M. Milliam, S. S. Iyengar, J. Tomasi, V. Barone, B. Mennucci, M. Cossi, G. Scalmani, N. Rega, G. A. Petersson, H. Nakatsuji, M. Hada, M. Ehara, K. Toyota, R. Fukuda, J. Hasegawa, M. Ishida, T. Nakajima, Y. Honda, O. Kitao, H. Nakai, M. Klene, X. Li, J. E. Knox, H. P. Hratchian, J. B. Cross, V. Bakken, C. Adamo, J. Jaramillo, R. Gomperts, R. E. Stratmann, O. Yazyev, A. J. Austin, R. Cammi, C. Pomelli, J. W. Ochterski, P. Y. Ayala, K. Morokuma, G. A. Voth, P. Salvador, J. J. Dannenberg, V. G. Zakrzewski, S. Dapprich, A. D. Daniels, M. C. Strain, O. Farkas, D. K. Malick, A. D. Rabuck, K. Raghavachari, J. B. Foresman, J. V. Ortiz, Q. Cui, A. G. Baboul, S. Clifford, J. Coislowski, B. B. Stefanov, G. Liu, A. Liashenko, P. Piskorz, I. Komaromi, R. L. Martin, D. J. Fox, T. Keith, M. A. Al-Laham, C. Y. Peng, A. Nanayakkara, M. Challacombe, P. M. W. Gill, B. Johnson, W. Chen, M. W. Wong, C. Gonzalez, and J. A. Pople, Gaussian 03, Revision B.05, Gaussian, Inc., Wallingford CT (**2004**).
125. N. Chakrapani, Y. M. Zhang, S. K. Nayak, J. A. Moore, D. L. Carroll, Y. Y. Choi, and P. M. Ajayan, *J. Phys. Chem. B* 107, 9308 (**2003**).
126. A. J. Lu and B. C. Pan, *Phys. Rev. B* 71, 165416 (**2005**).
127. F. Mercuri, A. Sgamellotti, L. Valentini, I. Armentano, and J. M. Kenny, *J. Phys. Chem. B* 109, 13175 (**2005**).
128. F. A. Cotton, G. Wilkinson, C. A. Murillo, and M. Bochmann, Advanced Inorganic Chemistry, 6th edn., John Wiley & Sons, Inc., New York (**1999**).
129. V. Hsieh, A. G. D. Crisci, A. G. Lough, and U. Fekl, *Organometallics* 26, 938 (**2007**).
130. C. R. Baar, H. A. Jenkins, J. J. Vittal, G. P. A. Yap, and R. J. Puddephatt, *Organometallics* 17, 2805 (**1998**).
131. S. S. Stahl, J. A. Labinger, and J. E. Bercaw, *J. Am. Chem. Soc.* 117, 9371 (**1995**).
132. M. Gajdoš, J. Hafner, and A. Eichler, *J. Phys.: Cond. Matt.* 18, 13 (**2006**).
133. H. Orita, I. Nakamura, and T. Fujitani, *J. Phys. Chem. B* 109, 10312 (**2005**).
134. V. Rosca, G. L. Beltramo, and M. T. M. Koper, *Langmuir* 21, 1448 (**2005**).
135. E. H. G. Backus, A. Eichler, M. L. Grecea, A. W. Kleyn, and M. Bonn, *J. Chem. Phys.* 121, 7946 (**2004**).
136. G. Natile, F. P. Intini, R. Bertani, R. A. Michelin, M. Mozzon, S. M. Sbovata, A. Venzo, and R. Seraglia, *J. Organomet. Chem.* 690, 2121 (**2005**).
137. G. Bernhardt, H. Brunner, N. Gruber, C. Lottner, S. K. Pushpan, T. Tsuno, and M. Zabel, *Inorg. Chim. Acta* 357, 4452 (**2004**).
138. M.-H. Baik, R. A. Friesner, and S. J. Lippard, *Inorg. Chem.* 42, 8615 (**2003**).
139. G. Novell-Leruth, A. Valcárcel, A. Clotet, J. M. Ricart, and J. Pérez-Ramírez, *J. Phys. Chem. B* 109, 18061 (**2005**).
140. U. J. Kilgore, X. Yang, J. Tomaszewski, J. C. Huffman, and D. J. Mindiola, *Inorg. Chem.* 45, 10712 (**2006**).
141. E. A. MacLachlan and M. D. Fryzuk, *Organometallics* 25, 1530 (**2006**).
142. E. M. Stuve and R. J. Madix, *J. Phys. Chem.* 89, 3183 (**1985**).
143. A. Hayashi, Y. Xie, J. M. Poblet, J. M. Campanera, C. B. Lebrilla, and A. L. Balch, *J. Phys. Chem. A* 108, 2192 (**2004**).
144. N. R. Avery, *Langmuir* 4, 445 (**1988**).
145. P. C. Stair and G. A. Somorjai, *J. Chem. Phys.* 66, 2036 (**1977**).
146. L. Menzel, A. A. Kosterev, R. F. Curl, F. K. Tittel, C. Gmachl, F. Capasso, D. L. Sivco, J. N. Baillargeon, A. L. Hutchinson, A. Y. Cho, and W. Urban, *Appl. Phys. B* 72, 859 (**2001**).

Received: 18 April 2008. Accepted: 17 October 2008.

REVIEW